THE AMERICAN MINERALOGIST
JOURNAL OF THE MINERALOGICAL SOCIETY OF AMERICA

Vol. 27 NOVEMBER, 1942 No. 11

APPARATUS FOR DIRECT MEASUREMENT OF LINEAR STRUCTURES

EARL INGERSON,
Geophysical Laboratory, Carnegie Institution of Washington.

It is not difficult to measure the angle and direction of pitch of a linear structure with a Brunton compass, if the outcrop is readily accessible, and the lineation is not too steep and can be seen in three dimensions. It must be seen in three dimensions, of course, for an accurate measurement to be made by any method. The direction of pitch is commonly measured by standing directly above the lineation and lining it up parallel to a side, or the slot, of the Brunton compass as it is held level. This amounts to projecting the lineation onto a horizontal plane and the direction is read directly on the compass. The angle of pitch is measured by placing the lower edge of the compass on the lineation and using it as a clinometer. There is always some uncertainty in the mental projection of the lineation onto a horizontal plane, and this uncertainty increases as the angle of pitch increases. Moreover, it is necessary to make two readings with the compass in different positions, which takes a great deal of time when many readings are being made.

On small outcrops that are accessible only with difficulty, or where the lineation is steep, a more accurate method is to measure the dip and strike of a plane containing the lineation, then measure the angle in the plane between the lineation and the dip or strike of the plane. Then a graphic solution, which is very simple with a stereographic net, gives the direction and angle of pitch of the lineation.

A simple illustration will serve to show how this is accomplished. Suppose that the dip and strike of an *s*-plane have been determined as N 56°W 70°NE. A lineation in the *s*-plane makes an angle of 69° with the strike of the *s*-plane, down to the northwest. Let the projection net represent the lower half of the projection sphere, and let the projection plane be horizontal, with customary map orientation. The construction is done on a piece of tracing paper placed over the net. Make an orientation arrow at the south pole of the projection and turn the tracing paper until the arrow points to 56°W. Now a great circle 70° from the

eastern margin of the projection represents the *s*-plane, and a point on this great circle 69° from the north pole of the projection represents the lineation. This part of the construction is shown in Fig. 1.

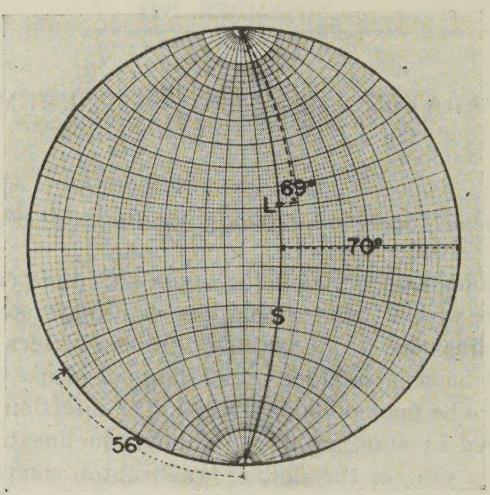

FIG. 1. Method of plotting on a stereographic projection an *s*-plane containing a lineation. Data: *s*-plane N 56°W 70°NE, lineation makes an angle of 69° with strike of *s*-plane, as measured in the plane, down to the northwest.

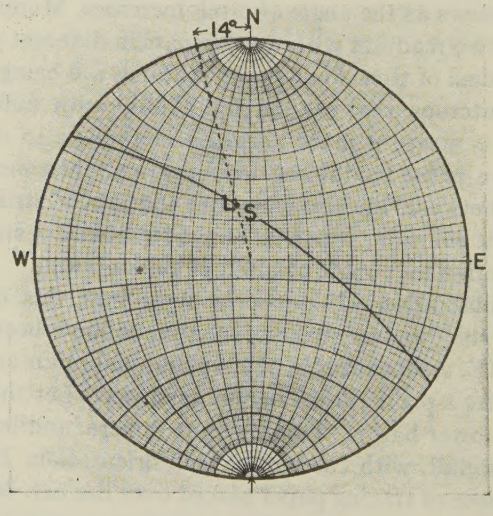

FIG. 2. Method of determining the direction of pitch of the lineation represented in Fig. 1.

To find the direction of pitch of the lineation the tracing paper is turned back to the zero point and a line is drawn from the center of the net through the point representing the lineation, to the periphery of the projection. This point indicates the direction of pitch, N 14°W in the example. Figure 2 shows this construction. The angle of pitch is determined by placing the point representing the lineation on the equator of the projection (Fig. 3) and reading the angle between that point and the periphery of the projection, between 61° and 62° in the example. Summary of data in the example: *s*-plane, N 56°W 70°NE; lineation ∧ strike of *s*-plane, 69°N; lineation N 14°W 61°+.

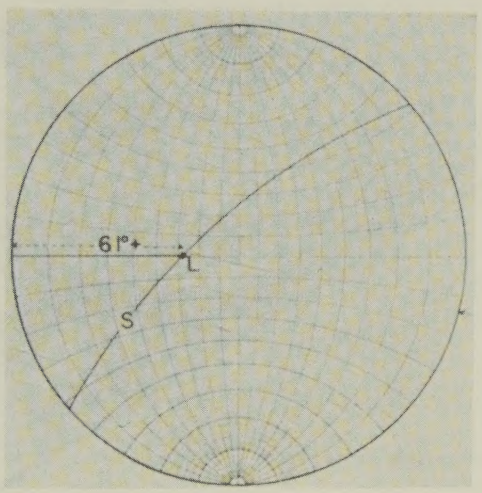

FIG. 3. Method of determining the angle of pitch of the lineation represented in Fig. 1.

While this method is more accurate than the other in many instances, it has the added disadvantages of requiring a third measurement, which must be made with a protractor, and of requiring a graphic solution. Besides taking more time, it does not give final measurements for comparison in the field.

A simple arrangement (Fig. 4) for reading the direction and angle of pitch with a single placing of the compass can save much time in taking a series of lineation measurements. It consists of a compass mounted with a graduated semicircle that is weighted so that it remains vertical; the compass is provided with a weighted pointer that keeps it horizontal. This arrangement is swung on pivots in a frame that has a straight edge that can be placed on, or parallel to, a linear structure

in the field. Direction of pitch is read on the compass, and angle of pitch is read on the vertical circle.

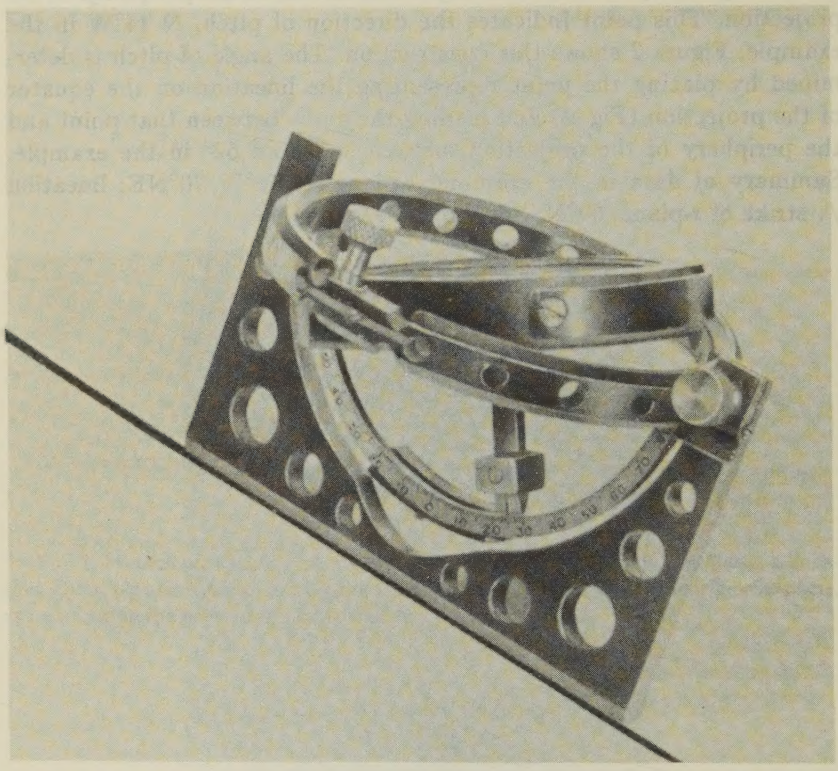

FIG. 4. Apparatus ("universal compass") for measuring geographic coordinates of a linear structure in three dimensions with a single placing of the compass.

The apparatus can be used on overhanging surfaces (Fig. 5) and on outcrops where no planar structure is apparent just as well as on the more commonly encountered type of outcrop. It was tried out underground by Mr. Glenn Waterman of the Idaho Maryland Mines Corporation, who reported that it was difficult to make readings above eye level, and suggested that a transparent bottom on the compass case would allow readings to be made from below without moving the instrument or using a mirror.

Dip and strike of a plane can be determined by measuring the dip just as a lineation is measured, and taking the direction normal to the direction of pitch as the strike of the planar structure. The vertical

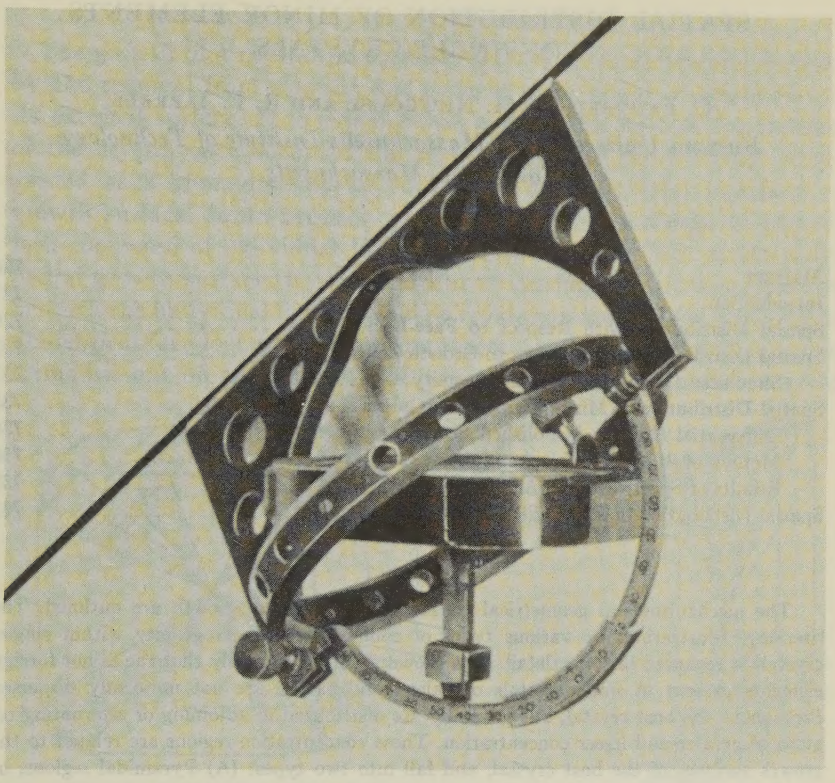

FIG. 5. Use of "universal compass" on an overhanging surface.

circle and weighted pointer are hinged so that the apparatus folds up and can be placed in a case no thicker and not much longer than that of an ordinary Brunton compass.

SPATIAL DISTRIBUTION OF MINOR ELEMENTS IN SINGLE-CRYSTALS

C. Frondel, W. H. Newhouse and R. F. Jarrell,
Harvard University and Massachusetts Institute of Technology, Cambridge, Massachusetts.

Contents

Abstract 726
Introduction 727
Spatial Distribution with Respect to Face-Loci 729
Spatial Distribution with Respect to Growth Zones 732
Simulated Compositional Heterogeneity 733
Spatial Distribution of Minor Elements in Galena 735
Differential Staining in Polished Section 736
Method of Spectrographic Analysis 738
Results of Spectrographic Analyses 739
Spatial Distribution of Minor Elements in Calcite 743

Abstract

The mechanism and geometrical consequences of crystal growth are outlined. The literature illustrating the various types of compositional heterogeneity within single-crystals is reviewed in some detail. It is shown spectrographically that the minor foreign elements present in single-crystals of galena and calcite are not uniformly dispersed throughout the host crystal, but generally are distributed in adjoining or alternating regions of greater and lesser concentration. These concentration-regions are related to the growth surfaces of the host crystal, and fall into two types: (A) Pyramidal regions, or face-loci, subjacent to particular faces on crystals bounded externally by several crystallographically different forms. The concentration differences arise in the unequal adsorptive capacity of the different forms on the growing crystal for the foreign element in question. (B) Alternating zones parallel to the external growth surfaces without any or marked selectivity as to different crystal faces. Growth zoning may have two origins: a roughly periodic variation in the rate at which foreign material is taken up by the host crystal in a closed system under the control of certain properties peculiar to growth surfaces, and a zoning occasioned by progressive variation in the composition of the crystallizing solution or in other outside factors.

The spectrographic work on galena revealed that both Ag and Si are relatively concentrated in the octahedral face-loci. Other minor elements, including Cu, Fe, Al, Cr, Ba, Sr, Ca and Mg, show significant quantitative variations within galena single-crystals but apparently without any special relation to the morphology. Staining of sectioned and polished single-crystals of galena reveals a complex internal structure outlined by relatively reactive, dark-stained, growth zones and face-loci. Correlated spectrographic examination indicates that the dark stained regions are relatively rich in Ag. Spectrographic examination of calcite single-crystals further illustrates the features of distribution found with galena. Significant compositional variations are found between successive growth zones in habit-invariant single crystals and between overgrown crystals of different habit. No special connection, however, could be traced between the morphology or the color of the crystals and any of the minor elements tested (Fe, Cu, Mn, Al, Sr, Mg).

Introduction

The growth of a crystal proceeds outwardly from an original nucleus by the removal from solution and ordered attachment of substance to its external surface. It is evident that every point now in the interior of the crystal once occupied the surface, and the crystal may be regarded as a three-dimensional locus of a solution/solid interface or growth surface. More precisely, a crystal is an assemblage of growth loci, composed of individual loci each subjacent to a face of the polyhedral growth surface. It is convenient to distinguish between *face-loci* beneath the individual faces of a single crystallographic form, and groups of identical face-loci, or *form-loci*, representing different crystallographic forms present on the crystal. The essentially two-dimensional internal

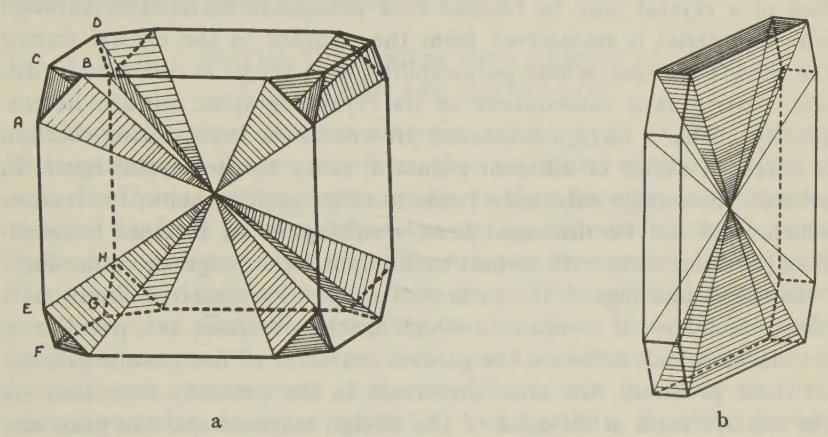

Fig. 1. Diagrammatic representation of form-, face-, edge-, and corner-loci. The isometric cubo-octahedron shown at the left is composed of: (A) two different form-loci, comprising the octahedral face-locus *ABCO* with its 8 analogues, and the cubical face-locus *ACDEFGHO* with its 6 analogues. (B) Two different edge-loci, comprising the octahedral edge-locus *ABO* with its 24 analogues, and the cubical edge-locus *CDO* with its 12 analogues. (C) One set of corner-loci, comprising *AO* and its 24 analogues. Compare Fig. 4*b*.

The holohedral orthorhombic crystal shown at the right contains 4 different kinds of form-loci, 5 different kinds of edge-loci, and 2 different kinds of corner-loci. The brookite crystal with a selective pigmentation of the face-loci of {001} shown in Fig. 2*a* has an identical habit.

bounding surfaces between adjacent face-loci also are loci, traced out by the edges of the crystal during its growth, and may be designated *edge-loci*. Similarly, the one-dimensional, line-like, juncture of three or more adjacent face-loci representing the successive positions during growth of the corners of the crystal are corner-loci. It is apparent that there may be different kinds of both edge- and corner-loci, cor-

responding to the crystallographically different kinds of edges and corners on the growth surface. The several types of loci here described are illustrated in Fig. 1.

It may now be considered that the surface of a crystal is both (1) heterogeneous, in that the surface itself is composed in general of a variety of unlike faces, edges and corners, each with different geometrical, chemical and physical properties, and (2) discontinuous, in the sense that the surface marks an abrupt boundary between two unlike phases or environments. Both the heterogeneity and the discontinuity of the crystal surface may act individually to impose non-uniform, spatial, characters on the distribution within the crystal of a foreign substance taken up by the crystal during its growth. In the first regard, the surface of a crystal may be likened to a permeable membrane, through which material is transferred from the solution to the crystal during the growth process, whose permeability, in a sense, is different in different parts as a consequence of its crystallographic surface heterogeneity. Thus, a foreign substance present in the crystallizing solution is offered a choice of different points of entry to the crystal itself. In general, the foreign substance tends to effect such a choice, for reasons which need not be discussed here, resulting in an internal compositional heterogeneity with respect to different form-, edge- or corner-loci.[1]

In the second regard, the surface of a crystal, considered simply as a phase boundary, is a region in which special processes act, peculiar to interfaces, which influence the general character of the growth process. Of these processes, the most important in the present connection are the relative rates of diffusion of the foreign material and the pure material from the solution to the crystal surface, the rate of crystal growth, and the dissipation of the heat of crystallization. The interaction of these processes causes a more or less crude periodicity in the rate at which the foreign material is taken up by the growing crystal, giving rise to an internal compositional heterogeneity with respect to concentric, shell-like, zones which parallel all of the growth surfaces. The growth of a crystal from pure solution probably also is periodic, but direct experimental evidence on this point is lacking.[2] It must also be remarked, that compositional zoning may be occasioned by bulk changes in the composition of the solution during the course of crystallization, or by changing equilibria in a solution of fixed bulk composition accompanying varia-

[1] An introduction to this problem can be gained from investigations by Bunn, C. W., *Proc. Royal Soc. London*, **141A,** 567 (1933); Buckley, H. E., *Zeits. Krist.*, **81,** 157 (1932); **80,** 238 (1931); **88,** 392 (1934); and Frondel, C., *Am. Mineral.*, **25,** 91, 338 (1940), on the adsorption of substance by certain faces only of growing crystals.

[2] See, however, the observations of Miers, H. A., *Phil. Trans.*, **202,** 459 (1904), on alum.

tion in external conditions. This aspect of the problem has been well discussed by Phemister (1) in the case of the zoning of the plagioclase feldspars. Zoning due to these causes may be superposed on a zoning due to properties of growth surfaces *per se*.

The present study is concerned with the spatial distribution within the host crystal of the so-called minor elements present in spectrographic amounts. Particular reference is made to galena and to calcite. Before the description of this work is entered, however, it may be of interest to review briefly some of the recognized examples of the growth-loci and zonal types of compositional heterogeneity, and to indicate the various phenomena by which a spatial distribution of foreign material may be evidenced. A limited review of observations in this general field has been given by Nothaft and Steinmetz (2).

Spatial Distribtion with Respect to Face-, Edge- and Corner-Loci

Perhaps the most familiar examples of this type of compositional heterogeneity are the so-called hour-glass segmental or sectoral types of color distribution within single-crystals. In these instances, a pigmenting material has been preferentially taken up, in solid solution or otherwise, by the faces of a particular crystal form during the growth of the crystal. The described instances among both natural and artificial crystals are very numerous. Particular reference may be made, however, to studies by Haberlandt and Schiener and others on the differential coloration of face-loci and growth zones in fluorite (3). A large literature on these phenomena also exists for barite (4) and brookite. Brookite crystals from Ellenville, New York, with a marked hour-glass pigmentation in certain form-loci are shown in Fig. 2; spectrographic analysis has shown that the dark regions contain relatively large amounts of Cb in substitutional solid solution for Ti. The spatial distribution of dyes within particular form-loci of crystals grown from solutions containing added dyes has been the subject of much investigation (5).

Spatial distribution with respect to form-loci also may be revealed in uniformly colored or in opaque and visually homogeneous crystals by appropriate means. Colorless crystals of K_2SO_4, $(NH_4)_2SO_4$ and some other substances when grown from solutions containing added radioactive ThB, ThX, or Po and then placed upon a wrapped photographic film give a radiograph which reveals a selective distribution of the substituted radioactive atoms within particular form-loci (6). Similarly, the uranium present in solid solution in natural crystals of various columbate-tantalates appears quite frequently to be selectively concentrated within particular form-loci in the crystal. Some examples are

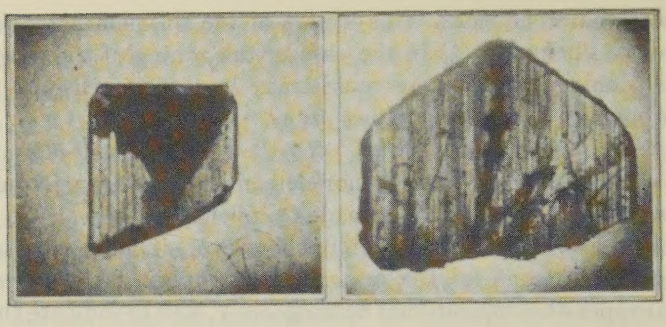

FIG. 2. At left is a photograph of a brookite crystal from Ellenville, New York, with a black selective pigmentation of the face-loci of {001}. The bottom half of the crystal is broken off. Growth zones parallel to (001) are present in the pigmented region. The vertical lines are striations. Spectrographic analysis shows that the dark material is high in Cb. The Cb is in isomorphous substitution for Ti. Arnold, W., *Zeits. Krist.*, **71**, 344 (1929), who cites many instances of selective pigmentation in brookite, also found by *x*-ray emission analysis that the dark material in crystals from Switzerland is high in Cb. At right is a brookite crystal from Tavetsch, Switzerland, with a narrow, selectively pigmented, face-locus of {001}. Magnification = 19×.

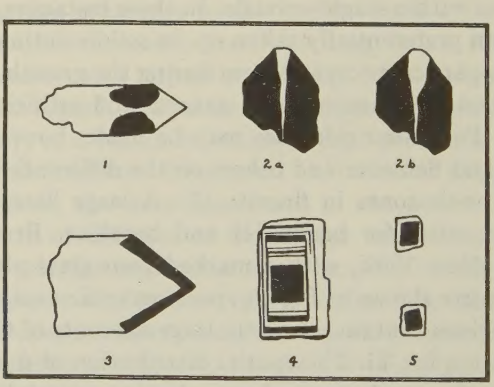

FIG. 3. Tracings of radiographs of oriented sections through single-crystals of various radioactive columbate-tantalates. No. 1 is a basal section through a blomstrandine crystal from Hitterö, Norway. No. 2*a* and 2*b* are succesive sections parallel {010} through a polycrase crystal from Marietta, South Carolina; the sections show a well-defined weakly-radioactive face-locus of {001}. No. 3 shows a zone of strongly radioactive material selectively disposed beneath the faces of {001} on a crystal of blomstrandine from Morefjaer, Norway. No. 4 illustrates a zonal structure in a basal section of samarskite from Uba, Minas Geraes, Brazil. No. 5 shows a zonal structure in basal sections of fergusonite from Satersdalen, Norway.

shown in Fig. 3 and are described in the caption. Numerous instances have been described of the selective luminescence of form-loci in single-crystals under excitation by ultraviolet light or otherwise. Gypsum

crystals from more than six localities have been found to show strong selective fluorescence in the face-loci of {111} (7). Certain calcite crystals from Terlingua, Texas, bounded by a scalenohedron and a rhombohedron, fluoresce selectively in ultraviolet light in the face-loci of the rhombohedron. Selective fluorescence of face-loci also has been observed in fluorite, apatite and apophyllite. The unlike sensitivity of the different forms on single-crystals of pyrite and some other metallic sulfides when used as radio-detectors apparently is connected with minor variations in the composition of the several form-loci (8). The chemical reactivity of crystals is, in general, sensitive to minor variations in composition, and chemical differences between form-loci may then be revealed in cut sections by etching or staining techniques. The compositional heterogeneity of galena single-crystals as revealed by differential staining is described on the following pages, and many further examples among opaque minerals are found in the literature (9, 10). The optical constants of crystals similarly may vary with variation in composition, and the optical heterogeneity with respect to form-loci of mixed crystals often is marked (11). A remarkable series of photographs have been published (12) of complex optical heterogeneities with respect to face-loci and growth zones in mixed crystals of the voltaite series. These effects are concomitants of chemical variations, and aften are accompanied by a differential coloration of the several parts. A concomitant hour-glass type of variation in both coloration and birefringence is found in certain ferroan epidote crystals (13), among other species, and is well known in the case of the titanian augites found in igneous rocks (14). It may also be expected that exsolution products should be more abundant in or localized in particular form-loci if these varied in their original content of dissolved foreign material. Examples of this type of distribution are known among artificially grown unstable mixed crystals (15), but unqualified instances apparently have not been recognized among natural crystals.

Compositional variation with respect to edge-loci and corner-loci is difficult to recognize because of the extremely small volume occupied by these regions within the crystal. Well-defined selectively colored edge-loci beneath the terminating rhombohedron are sometimes found in zoned tourmaline crystals from Madagascar (16). Differentially colored edge-loci also appear in some published photographs of sectioned fluorite crystals (17). Some of these instances may be only of extremely narrow form-loci. Substituted atoms of radioactive ThB in single crystals of lead chromate are relatively concentrated in the edge-loci (18). The edges and corners of crystals, including here surface imperfections arising in lineage or mosaic structures and striations, are, as is well known,

regions of great adsorptive capacity as compared to plane surfaces, and edge- and corner-loci can be expected to be regions of marked compositional heterogeneity. While such heterogeneity would be of little consequence on the bulk composition, it might be of marked effect on the magnetic and especially the electrical properties of the crystal.

Spatial Distribution with Respect to Growth Zones

This type of compositional heterogeneity has been variously designated as zonal growth, compositional zoning, growth banding or phantom banding. The zones may be continuous around the crystal or, if there is a selective distribution of the foreign material with respect to form-loci, be confined to such loci. An instance of the latter kind in brookite is shown in Fig. 2. The zones often are continuous around the crystal but are of different thickness if different form-loci. Zoning frequently reveals a progressive or abrupt change of habit during the growth of the crystal. Changes in shape (distortion) due to growth in a solution current also may be revealed (19, 43). The thickness of growth zones at opposite ends of a polar crystal axis may be expected to be unlike, due to the intrinsically unequal rates of growth in opposite senses of the axis, and have been so found in tourmaline. Growth zoning is characteristic of mixed crystals in an isomorphous series, such as the smaltite-chloanthite series, ferroan sphalerite, the ferberite-hübnerite series (20), the plagioclase feldspars (1), pyromorphite (32) and many others. Contrary to what is probably generally believed, there is not always a progressive change in composition outwardly in zoned mixed crystals, such as would result from a regular variation in the composition of the crystallizing solution. Usually the zones are simply repeated periodically in a more or less definite ratio, and the average composition of any region of appreciable thickness in the crystal is a constant; this is the type of zoning impressed by properties inherent in the growth mechanism of crystal surfaces. Zoning of the latter type is typical of crystals containing adsorbed colloidal particles of a foreign pigmenting substance, such as amethyst (21) and crystals containing dyes.

In transparent crystals zonal growth also may be revealed by variation in optical properties and, in both opaque and transparent crystals, by etching or staining techniques. The unequal fluorescence in ultraviolet light of growth zones in diamond crystals has been recently described (22). The selective luminescence in this and in similar instances in fluorite and calcite definitely appears to be due to minor variations in composition of the several zones. Certain calcite crystals investigated

by Headden (23) exhibited internal color zones; these zones exhibited differential phosphorescence when exposed to direct sunlight or to x-rays, thermoluminesced differentially when heated, and exhibited differential triboluminescence. In one instance, the zones were shown to differ in the kind and content of rare-earths present in very small amounts in solid solution in the calcite. Fluorite very frequently shows selective fluorescence in ultraviolet light with respect to growth zones. Some fluorite crystals exhibit zonal phosphorescence (24) after exposure to sunlight, and an instance has been described of zonal thermoluminescence (25) when heated after exposure to radium rays. The thermoelectric potential of pyrite is influenced by zoning in the crystals, and in one instance the variation was found to be due to differences in composition of the zones (26). The zonal distribution of radioactive material in single-crystals of various columbate-tantalates already has been illustrated (Fig. 3). A similar distribution occurs in artificial crystals containing radioactive impurities (6). Very frequently, compositional zoning is revealed or accentuated by differential chemical alteration of the zones; the alteration of the calcic zones of plagioclase crystals to zoisite, etc., and the differential solution and alteration of longitudinally zoned tourmaline crystals are familiar examples. The oxidation of magnetite to hematite or maghemite usually takes place preferentially along particular growth zones within the magnetite crystal (27), and this presumably reflects a compositional heterogeneity. The replacement of crystals often is influenced by zoning; for instance, zoned pyrite replaced by chalcocite (32; Fig. 26). Exsolution products are sometimes restricted to particular growth zones. Thus, NaCl forms a limited range of unstable mixed crystals with AgCl, and the mixed crystals contain zones alternately rich and poor in Ag; the Ag-rich zones show anomalous birefringence and on standing become turbid due to the deposition of minute parallely oriented crystals of AgCl (15).

Simulated Compositional Heterogeneity. Inclusions in Crystals. Internal structures which simulate both the zonal and the growth-loci types of compositional heterogeneity may be observed in crystals. The closely spaced, white and opaque growth zones in otherwise colorless barite crystals have been found in one instance (28) to be due to the presence of myriads of minute empty cavities. Zonally arranged minute fluid cavities have been observed in barite crystals from many other localities (44). A micro-composite structure may be present in certain form-loci only of Rochelle-salt crystals (29) giving rise to a turbidity which simulates the hour-glass type of compositional heterogeneity; the presence of these composite form-loci greatly enhances the piezo-electric efficiency

of the crystals. A similar turbidity of certain growth-loci only, due to the scattering of light by crystal flaws and inclusions, has been observed in artificial halite (30) and $Na_2S_2O_3$ (31) crystals.

It also has been observed that inclusions ranging in size from dust-like particles to macroscopic crystals have been included in great numbers during particular stages of growth of the host crystal. Turbid or pigmented zones of this nature may closely simulate a true compositional heterogeneity. In some instances, such as the microscopic ilmenite (?) inclusions in the accessory apatite of igneous rocks, the included material appears to have been available in continuous supply throughout the growth of the host crystal but nevertheless was taken up in a discontinuous, roughly periodic, fashion. The mechanism proposed (33) to account for the periodicity is similar in its essentials to that which acts in true compositional zoning. The so-called capped quartz crystals, consisting of repeated separable shells parallel to the terminating rhombohedral faces, apparently owe their origin (34) to the periodic deposition and inclusion of clayey or micaceous material which locally reduces the cohesion of the crystal. Zonally separable barite crystals of similar origin have been described, and the cleavage or parting induced in certain artificial crystals by the adsorption of dyes also appears to be of this nature. In other instances, as in drusy crystallization in cavities from traversing solutions containing suspended particles, the included material seems to have been available only intermittently during the course of crystal growth. Deposition of scattered crystals of another mineral species upon the surface of a host crystal with concomitant growth of the host crystal gives rise to what may be termed buried overgrowths. Crystal inclusions of this origin may be crystallographically oriented to the host crystal, or be selectively disposed with respect to crystal forms or to edges and corners (35). An arrangement of minute inclusions along edge-loci has been described in zircon, garnet, gypsum and other species (36), and tiny pyrite crystals have been found arranged along certain corner-loci in calcite crystals.

In the so-called anomalous mixed crystals, two structurally related but distinct crystal phases are inter-crystallized in an intimate, oriented fashion. Such bodies characteristically exhibit zoning on a closely repeated, microscopic, scale. Successive zones are alternately rich and poor in one of the phases. The zoning, and the circumstance of formation of the intergrowth itself, is a consequence of the periodic interaction of diffusion processes acting at the growth surfaces, and stands in closest relation to the zoning observed in true mixed crystals. The different expression of the interface processes in the two cases is a result of phase equilibria in the solution: in the one case the foreign atoms can be housed by isomorphous substitution in a single-phase host crystal, and the

periodic variation in concentration of the foreign atoms at the interface gives rise to compositional (isomorphous) zoning; in the other case, the variation in concentration at the interface periodically oversteps a phase boundary and a layering of phases rather than of isomorphous zones results. The zones in anomalous mixed-crystals may be continuous around the crystal, but sometimes the intergrown phase which causes the zoning is restricted to particular form-loci.

It is hoped that the foregoing discussion has emphasized the point of view that crystals are heterogeneous and discontinuous structures not only with respect to their surface geometry, as is ordinarily considered, but also with respect to their internal characters. Crystals have an internal morphology, defined by chemical and physical properties rather than by geometrical characters. This internal heterogeneity can be revealed by appropriate means, and can be applied variously to problems of crystal- and mineral-genesis.

Spatial Distribution of Minor Elements in Galena Single-Crystals

The spatial distribution within single crystals of galena of Ag, Cu, Mg, Al, Fe, Si and other minor elements was investigated by correlated spectrographic and polished section methods. The galena crystals employed were single euhedral individuals bounded externally by two or more crystallographically different forms. A description of the specimens is given in Table 1.

Table 1. Locality and Habit of Galena Crystals

Number	Locality	Habit
1	Telhadela, Portugal	{001} and {111} same size
2	Mina da Mathada, Portugal	{001} and {111} same size
3	Mina da Braçal, Portugal	{001} and very small {111}
4	Alston Moor, England	{001} and small {111}
5	Breckenridge, Colorado	{001} and small {111}
6	Joplin, Missouri	{111} and small {001}
7	Bingham, Utah	{001} and small {111}
8	Summit Co., Colorado	{001} and small {111}
9	Silesia	{001} and small {111}
10	Joplin, Missouri	{001} and very small {111}
11	Joplin, Missouri	{001} and {111} same size
12	Webb City, Missouri	{001} and {111} same size
13	Joplin, Missouri	{001} and small {111}
14	Derbyshire, England	{111} and small {001}
15	Ottawa Co., Oklahoma	Octahedra overgrowing cubes (separate crystals)
16	Neudorf, Saxony	{001}, {011} and small {111}

Differential Staining in Polished Section. Interior sections oriented parallel to {001} of the galena crystals were polished and treated with a solution containing 1 volume conc. HNO_3 to 8 volumes H_2O. Several sections usually were cut at different levels in the same crystal. A differential staining was obtained which clearly revealed that the crystals were internally partitioned into regions of greater and less chemical reactivity. The appearance of some representative stained sections is shown in Fig. 4. Unimportant detail was eliminated in drawing some of

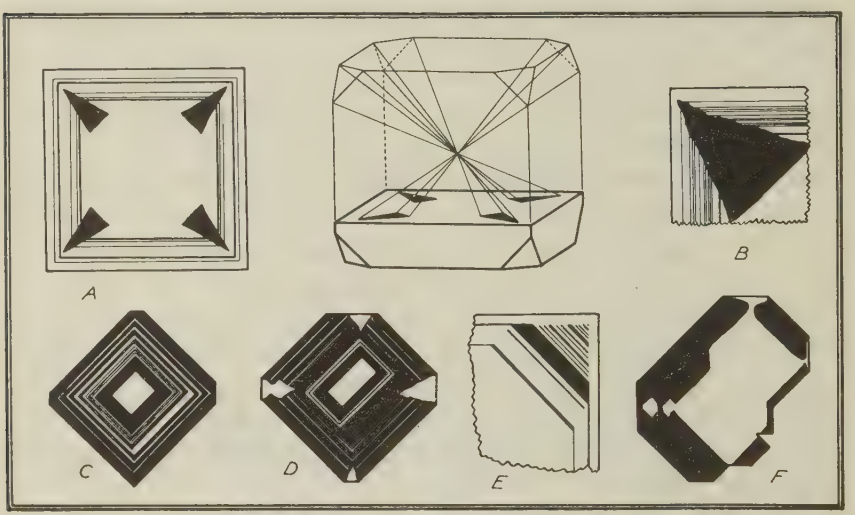

FIG. 4. Differentially stained sections of galena revealing face-loci and growth zones. The sections are parallel (001) and the separate crystals are parallely oriented. The dark areas and zones are relatively reactive, Ag-rich, galena. Section *A* is a shallow cut through a large cubo-octahedron of galena from Joplin. Triangular areas are exposed which are seen from the accompanying sketch to represent the face-loci of {111}. Section *B* is one corner of a large cube and exhibits both a face-locus of {111} and growth bands parallel {001}. Growth bands parallel {111} in an octahedral crystal are shown in section *C*. Section *D* is a crystal from Mina da Mathada, Portugal, with Ag-poor face-loci of {001} and octahedral growth zones in a dominantly octahedral crystal. Section *E* shows an enlargement of growth zones in a {111} face-locus of a cubo-octahedron. Section *F* shows a distorted cubo-octahedron with Ag-poor face-loci of {001}.

the figures and minor differences in intensity of the stain are not distinguished. The dark areas in the drawings represent the relatively reactive, dark-stained, portions of the crystals. These portions were found by spectrographic analyses, described beyond, to be distinguished by a relatively high content of Ag.

The spatial distribution of the Ag in the crystals illustrates both the zonal and the face-loci types of arrangement previously described. The Ag tends to enter solid solution preferentially via the growth faces of {111}. The Ag presumably substitutes for Pb atoms. In some sections no selectivity is shown between the several form-loci, but a zonal distribution appears always to be present. The zones may be confined to particular form-loci or be continuous around the crystal. The zones sometimes die out laterally, or are more strongly developed on one side of the crystal due to growth in a current (19). Relatively broad bands of Ag-rich material probably are composed of a multitude of closely spaced, extremely narrow, zones. The size and shape of the several equivalent face-loci as they appear in a given section may be quite varied, but their chemical reactivity and Ag-content always appears to be identical. It is important in interpreting the sections to visualize the several form-loci in three dimensions. Difficulties arise if the habit of the crystal has varied during growth, or if the form-loci are asymmetrically arranged due to an unequal development of the bounding faces. The relations between face-loci as revealed in irrationally oriented sections may be especially confusing. In sections parallel {001}, growth zones arranged parallel to the lateral cube faces are perpendicular to the plane of the section, but in the interior of the section, where the roots of the face-locus of the cube face parallel to which the section was cut are exposed, the zones are parallel to the plane of the section. Two sections cut at right angles through the same crystal are especially useful in interpreting the relations of the growth zones and face-loci.[3]

Several earlier observers also have recognized an internal partitioning of galena crystals of the nature here described. Becke (37) found an often "wonderfully delicate" zonal structure to be revealed by the action of hot HCl on cleavage sections. Specimens from Pribřam, Bohemia, contained inclusions of minute (0.01–0.001 mm.) unidentified needle-like crystals which were oriented to the galena and which were confined to particular growth zones; this may be an instance of localized exsolution. Recently, Fackert (38) has made a study of the internal *Gefügeausbau* of many galena crystals. His photographs of polished and differentially etched crystals strikingly reveal a distribution of relatively reactive galena with respect to growth zones and to face-loci. A mixture of HNO_3 and absolute alcohol was used as the etching reagent. The chemical

[3] Statements made in a previously published abstract by the authors, *Am. Mineral.*, **26**, 197 (1941), that Ag becomes more abundant in the crystals during the later stages of growth and that the early stages of growth usually were marked by an octahedral habit are not now considered sufficiently substantiated.

composition of the crystals was not investigated. Photographs of zoned galena crystals also are given by other authors (9, 10).

Method of Spectrographic Analysis. The analyses were made on the Wadsworth grating spectrograph of the Cabot Spectrographic Laboratory of the Department of Geology, Massachusetts Institute of Technology. The method used was that of the carbon arc cathode layer (39), with microphotometer readings of the line densities. All samples were mixed with three parts of carbon powder to ensure smoother burning. The load for each exposure weighed about 10 mg. The lower electrodes containing the sample were National Carbon Special Spectrographic Carbons, $\frac{3}{16}''$ diameter turned down to 3 mm. diameter for a distance of 5 mm. from the end, with a 1.5 mm. hole drilled to a depth of 6 mm. The upper electrodes were National Carbon Spectroscopic Graphites, $\frac{3}{16}''$ diameter. The current supply was 220 D.C. with ballast resistance and inductance to limit the current to about 7.5 amperes. The voltage across the terminals fluctuated between 50 and 60 volts. The cathode layer was projected on a $\frac{1}{8}''$ diaphragm which in turn was focused on the collimating mirror of the spectrograph.

It proved to be difficult to obtain a suitable internal standard which either did not already occur in the samples in appreciably irregular amounts or did not contain considerable amounts of the elements to be analyzed. Accordingly, a variation of the usual internal standard method was employed, similar to the technique long used to determine the relative intensities of lines of widely different wave-length. Several weak Pb lines were used as internal standard lines and all analysis lines, some as much as 1000 Å away, were compared with them. In order to obtain $\log \frac{\text{intensity analysis line}}{\text{intensity Pb line}}$ the densities of the Pb lines were converted into logarithm relative intensities by a characteristic curve for that wave-length made up from a stepped sector disc exposure of an Fe arc, and were then subtracted from the logarithm relative intensities of the analysis lines determined from their own characteristic curves. Since the logarithm relative intensity of each line was read from its own curve, the effect of variation of contrast with wave-length was compensated for to a first degree, as it would be by restricting the wave-length separation of the standard and analysis line and reading both from the same curve.

The values of $\log I$ obtained by subtracting lines read on one curve from lines read on another naturally depends not alone on the individual readings but also on the separation of the characteristic curves themselves. This in turn is, of course, a factor of the relative intensity in the source of the Fe calibration lines used and, because of the reciprocity law failure of the emulsion, of the intensity level of the exposure. For this reason the arc conditions and exposure times of the Fe sector exposures were carefully reproduced. Even then, the separation of the characteristic curves was found to vary slightly from film to film. Accordingly, the results were brought to a uniform basis by adding to or subtracting from the results on each film an amount equivalent to the difference between the separation of the curves for that film and the separation of the same curves for another film taken as standard. These separations were measured at a blackening level of $d = 1.0$. Since increased development has a more pronounced effect on the slope of the characteristic curve at higher wave-lengths, there is a second order error introduced by variations in development conditions, even after the curves have been brought to a consistent basis for $d = 1.0$. Development conditions were therefore reproduced insofar as possible. Three or four independent analyses were run for each sample, and the results were averaged. The resultant accuracy was not as great as that normally obtained under more favorable conditions. The average for $\log I_A/I_{Pb}$ for samples on the same film may be considered reliable for purposes of comparison to ± 0.05 in the case of Ag and ± 0.10 for the other elements.

The majority of the results were somewhat better than this. Comparisons from film to film are not so reliable, with the uncertainty at times as great as ± 0.10 for Ag and ± 0.20 for the others. For this reason the exposures for the material from the {001} faces were always made on the same film as the material from the {111} faces of the same crystal.

Results of the Spectrographic Analyses. The galena crystals were sampled by drilling out material from individual octahedral and cubical face-loci. A $\frac{1}{8}''$ hardened steel metal-working drill on a motor-driven flexible hand mounting was employed. A steel hand pick was used in sampling polished sections. Material taken from the faces of the several forms of a single-crystal should be spectrographed individually and not as an aggregate sample in order to recognize chance errors such as would be introduced by cutting into a foreign inclusion or by penetrating into an adjacent face-locus or growth zone.

The analyses made on the drilled samples are reported in Table 2. The larger numbers in the table denote larger amounts; thus, in Crystal 1, the octahedral face-loci contain more Ag and more Cu than do the cube-face loci. The limits of error for purposes of comparison are ± 0.05 for Ag and ± 0.10 for the other elements reported. Results marked *a* denote an absence of the element tested.

Comparison of the results for the octahedral and cubical faces shows that in the great majority of instances there is a difference beyond the limits of error in the content of the minor elements between the respective form-loci. In other words, the minor elements are not, in general, uniformly distributed within the host crystals. This is true for all of the elements tested. Further, there is clear evidence that some of the elements, at least, tend to be selectively concentrated in particular form-loci. Silicon is contained in greater amounts in the face-loci of {111} in 13 of the 15 crystals which contained this element; but in 4 instances the excess of Si in the {111} loci is not above the experimental error. Silver also appears to be relatively concentrated in the octahedral face-loci. Although half of the crystals examined contained an excess of Ag in the cube face-loci, only in one instance is the amount significantly greater than the experimental error, while of the other half, which contain Ag in excess in the octahedral face-loci, 7 of the 8 crystals contain a significant excess of this element.

It must be remarked, however, that the analytical results given in Table 2 were intended to represent the bulk or average composition of the face-loci, and thus do not necessarily indicate the maximum differences in composition between the dark, relatively reactive, galena and the ordinary galena as recognized in polished section. This is obviously the case for the individual face-loci may themselves be zoned, and hence, in a sense, diluted, or, as in other cases, the dark galena does not pre-

TABLE 2. RESULTS OF SPECTROGRAPHIC ANALYSES OF GALENA

Specimen	Form	Ag	Cu	Si	Mg	Al	Ca	Fe	Cr	Ba	Sr
1	111	1.10	−.18	−.47	.62		.92	.46	−.21		
	001	.80	−.62	−.76	.59		.83	.18	−.45		
2	111	1.09	.22	.49	.84	−.12	1.43	−.38	*a*	.42	−.42
	001	.98	.45	−.16	.61	−.70	1.00	−.72	*a*	.41	−.58
3	111	.85	.35	.19	.53	−.60	1.06	−.60	*a*	.36	−.80
	001	.93	−.31	−.30	.42	−.60	1.28	−.60	*a*	.59	*a*
4	111	.63	−.70	−.76	−.16		1.02	−.39		*a*	*a*
	001	.68	−.34	−.38	.24		1.26	−.06		*a*	*a*
5	111	1.36	.46	*a*	.33	−.34	1.14	−.39	*a*	.52	*a*
	001	1.34	.40	*a*	.32	−.51	1.10	.39	*a*	.54	*a*
6	111	−.31	−.23	−.01	.16			−.32	*a*	*a*	*a*
	001	−.24	−.13	−.08	.59			−.24	*a*	*a*	*a*
7	111	−.03	.92	.72	*a*		1.03	.88	*a*	−.14	*a*
	001	−.34	.68	.67	*a*		.84	1.15	*a*	−.38	*a*
8	111	1.64	.68	.40	.75		1.29	−.03	*a*	−.36	*a*
	001	1.73	.45	.08	.61		.74	.12	*a*	−.42	*a*
9	111	1.67	.11	.51	.99		1.36	.63	*a*	−.33	
	001	1.69	.37	.33	1.08		1.53	.30	*a*	−.30	*a*
10	111	−.03	−.38	−.33		.65		−.51	−.44	*a*	
	001	−.37	−.01	−.51		−.40		−.46	−.39	*a*	
11	111	−.06	−.38	.03		.66		−.38	−.42	*a*	
	001	−.22	.29	−.06		−.64		1.08	−.37	*a*	
12	111	.10	.10	.10	.16	−.33		−.26	−.51	−.39	
	001	−.03	−.03	−.35	.02	−.64		−.50	−.66	−.51	
13	111	−.20	−.20	.71	.45	−.28		.17	−.50	−.36	
	001	−.13	−.13	.40	.50	−.19		.29	−.50	−.39	
14	111	.89	.94	−.14	.03	−.80		−.29	*a*	*a*	*a*
	001	.95	1.01	−.17	.38	−.45		.09	*a*	*a*	*a*
15	111	−.96	−.51	−.82	−.07	.15	1.15	−.94	*a*	*a*	*a*
	001	−.34	−.61	.00	−.26	.13	.74	−.95	*a*	*a*	*a*
16	111	1.56	−.51	−.47	−.18	.23	.73	−.95	*a*	*a*	*a*
	001	1.56	−.61	−.48	−.29	.15	.52	−.99	*a*	*a*	*a*
	011	1.54	−.50	−.51	1.18	.19	.75	−.74			

ponderate in face-loci of a particular kind. The data of Table 2 thus probably possess minimum contrast. The maximum differences in composition between the dark and the ordinary galena are more accurately represented by the additional analyses reported in Table 3, following. These

TABLE 3. SPECTROGRAPHIC ANALYSES OF "DARK" AND "ORDINARY" GALENA

Number	Kind	Ag	Cu	Al	Mg	Si
6	Ord.	49.0	−45.3	−91.5	−16.6	
	Dark	70.5	−53.3	−26.8	3.5	
9	Ord.	36.75	−53	−54.25	26	
	Dark	64.25	−31	−64	69.5	
10	Ord.	−25.5	−55		11	
	Dark	3	−56.75		−10.75	
13	Ord.	−32	−44.75		10.5	*a*
	Dark	3.5	−30		*a*	18

samples were taken from selected polished and stained sections which exhibited relatively large and well-defined growth-zones and octahedral face-loci composed of dark-stained galena. Silver is uniformly present in significantly greater amounts in the dark galena, as is Si in the single determination made of this element. No systematic distribution is shown by the other elements reported. A ten-fold enrichment in Ag in the dark as compared to the ordinary galena was reported elsewhere (19) for another specimen, from Joplin, not included in this study. The amount of silver present in these galenas was estimated as never above 0.1 weight per cent, with the majority containing between 0.01 and 0.0001 per cent. The results of the analyses taken as a whole clearly indicate that the octahedral face-loci (to which the dark galena is relatively confined) are relatively rich in both Ag and Si. The Ag presumably is contained in isomorphous substitution for Pb. The manner in which the Si exists in the crystal, as discrete Si atoms, as SiO_4 groups or perhaps as colloidal particles of SiO_2, together with the housing mechanism itself, is entirely problematic. The mechanism by which the Ag and the Si were selectively distributed during the growth of the crystal between the octahedral and cubical face-loci constitutes a separate problem.

In connection with the enrichment of the octahedral face-loci in Ag and Si, it is interesting to note that octahedral crystals of galena long have been thought to be especially rich in Ag or to occur particularly with

silver ores. This correlation was first made by Werner in 1774, who stated (40) that

"Uebrigens scheint mir, so viel ich bemerkt habe, der mehrere oder wenigere Silbergehalt an der Verschiedenheit der Krystallisationen des Bleiglanz Ursach zu kenn, so, dass die Krystallisation desselben, wenn er mehr Silber halt, octahedrisch, und wenn er weniger halt, wurfelisch ist."

Jameson in 1820 remarked (41) that octahedral crystals were typically associated with silver ores, and others have made similar observations. This correlation of octahedral habit with silver content may be well founded, inasmuch as an adsorption of a foreign material by particular faces of a growing crystal, as of Ag by the octahedral faces of galena, ordinarily results in the development of those faces as the dominant habit. Recent studies (42) of the crystal habit of galena in relation to the paragenesis of the mineral suggest that octahedral and cubo-octahedral crystals usually occur with tetrahedrite, sphalerite, calcite and cubical crystals with quartz. Much work remains to be done, however, before any generalities can be drawn in these regards.

Table 4. Locality and Habit of Calcite Crystals

Number	Locality	Habit
1*a*	Joplin, Missouri	Scalenohedral crystals. Violet zone.
1*b*		Yellow-brown zone.
2*a*	Loughborough township, Ontario	Deep violet zone parallel {10$\bar{1}$1}
2*b*		Almost colorless zone parallel {10$\bar{1}$1}
3*a*	Rossie, New York	Violet zone parallel {10$\bar{1}$1}
3*b*		Almost colorless zone parallel {10$\bar{1}$1}
4*a*	Andreasberg, Saxony	Crystal tabular {0001}. Face-locus of {0001}
4*b*		Face-loci of lateral steep rhombohedron
5*a*	Tsumeb	Colorless outer zone {21$\bar{3}$1}
5*b*		Pale yellow interior zone {21$\bar{3}$1}
6*a*	Galetta, Ontario	Violet zone parallel {10$\bar{1}$1}
6*b*		Colorless zone parallel {10$\bar{1}$1}
7*a*	Locality unknown	Zoned crystal with habit change. 7*a* = inner colorless {10$\bar{1}$1}
7*b*		7*b* = outer pale brown {01$\bar{1}$2}
8*a*	Terlingua, Texas	Separate overgrown crystals. 8*a* = early yellow crystals {02$\bar{2}$1}
8*b*		8*b* = late colorless crystals {01$\bar{1}$2}
9	Kelley's Island, N. Y.	Crystal pyramidal {8.8.$\bar{16}$.3}; bulk sample.
10*a*	Terlingua, Texas	Complex zoned crystal. 10*a* = outer yellowish fluorescent zone
10*b*		10*b* = inner colorless non-fluorescent zone

Spatial Distribution of Minor Elements in Calcite Single-Crystals

Single-crystals of calcite were investigated along the same lines as was galena. Samples were taken symmetrically from different form-loci, and from growth-zones apparent within the crystal by reasons of color differ-

Table 5. Results of Spectrographic Analyses of Calcite

Number	Mg	Cu	Al	Fe	Mn	Sr
1*a*	.23	−.12	−.39	−1.07	− .13	− .42
1*b*	.23	−.60	−.21	−1.04	.44	.28
2*a*	.49	.02	−.18	− .42	.60	.21
2*b*	.23	−.79	−.35	− .93	1.00	.30
3*a*	.12	−.20	−.06	− .98	.51	.02
3*b*	−.49	.26	−.18	−1.17	− .29	.10
4*a*	−.03	−.34	−.24	− .95	.28	.01
4*b*	−.18	−.47	−.10	−1.00	.28	.18
5*a*	.12	−.70	−.03	−1.24	−1.01	−1.14
5*b*	.07	−.65	−.20	−1.26	−1.07	.26
6*a*	−.32	−.53	−.38	− .98	− .19	.03
6*b*	.14	−.35	−.38	− .56	.66	.24
7*a*	.04	−.51	−.38	− .33	1.06	.90
7*b*	.09	−.29	−.08	− .28	.61	.40
8*a*	.16	−.66	−.09	.28	.03	.70
8*b*	.16	−.61	−.06	.45	− .14	.48
9	.14	−.40	−.25	− .99	− .48	− .05
10*a*	.10	−.74	.58	− .50	− .33	.36
10*b*	.10	−.79	−.10	− .83	.00	.43

ences. The transparency of the mineral is a valuable aid in controlling the sampling. Descriptions of the specimens examined are given in Table 4. The results of the spectrographic analyses are listed in Table 5. The limits of error are ± 0.05 for Mg, ± 0.10 for Sr and ± 0.15 for Al, Fe, Mn and Cu. The results of the analyses clearly show that the minor elements are not uniformly distributed within the host crystal. This is true both for different form-loci and growth-zones in the same crystal and for separate generations of calcite crystals present on the same specimen. Due to

the simple habit and limited number of specimens examined it is not possible to trace any special connection between a minor element and particular form-loci, such as was found with galena. Such a relation may well exist, however, and is in fact to be inferred from observations such as the differential luminescence phenomena previously remarked and the known responsiveness of the habit of artificial calcite crystals to particular impurities in the crystallizing solution. Examples also are known of the selective coloration of form-loci in both calcite and aragonite.

There appears to be no definite correlation between the color of successive growth zones in the crystals and the content of minor elements. The violet and lilac colors of many calcites are known, however, to be due to the presence of rare-earths, and in some instances (23) the percentage and kind of rare-earths in successive growth zones has been shown to be different.

References

1. Phemister, J.: *Mineral. Mag.*, **23**, 541 (1934).
2. Nothaft, J., and Steinmetz, H.: *Chemie der Erde*, **5**, 225 (1930).
3. Haberlandt, H., and Schiener, A.: *Zeits. Krist.*, **90**, 193 (1935); Steinmetz, H.: *Zeits. Krist.*, **61**, 380 (1925); Drugman, J.: *Mineral. Mag.*, **23**, 139 (1932); Kenngott, G. A.: *Akad. Wiss. Wien, Sitzber.*, **11**, 605 (1853), *ibid.*, **13**, 481 (1854).
4. Ito T.: *Beitr. Min. Japan, n.s.*, **2**, 124, Pl. 8 (1937); Ardagh, E. G. R., *et al.: J. Chem. Soc. London, "Chem. & Indust."*, **53**, 1035 (1934); Sweet, J. M.: *Mineral. Mag.* **22**, 257 (1930); Pelikan, A.: *Min. Milth.*, **16**, 1 (1897).
5. Frondel, C.: *Am. Mineral.*, **25**, 91 (1940); Buckley, H. E.: *Zeits. Krist.*, **88**, 381 (1934), *ibid.*, **91**, 375 (1935); Buckley, H. E., and Cocker, W.: *Zeits. Krist.*, **85**, 58 (1933); France, W. G., and Rigterink, M. D.: *Jour. Phys. Chem.*, **42**, 1079 (1938).
6. Hahn, O., Käding, H., and Mumbrauer, R.: *Zeits. Krist.*, **87**, 387 (1934).
7. Josten, A.: *Cbl. Min.* (**1930**), 432. Figs. 1, 2.
8. Gaubert, P.: *C. R.*, **182**, 143 (1926); Hawkins, A. C.: *Am. Mineral.*, **11**, 164 (1927).
9. Schneiderhöhn, H., and Ramdohr, P.: *Lehrb. der Erzmikr.*, Berlin, **2**, Figs. 82, 91, 92, 101, 102, 112 (1931).
10. Van der Veen, R. W.: Mineragr. and Ore Dep., The Hague, **1**, Figs. 24, 25, 26, 56, 57, 57*a*, 100, 123 (1925).
11. Bunn, C. W.: *Proc. Royal Soc. London*, **141A**, 567 (1933).
12. Gossner, B., and Bäuerlein, T.: *Jb. Min., Beil.-Bd.* **66**, 1 (1932).
13. Shannon, E. V.: *Proc. U. S. Nat. Mus.*, **66**, 57, Fig. 7 (1924).
14. Holzner, J.: *Zeits. Krist.*, **87**, 1 (1934); Pelikan, A.: *Min. Milth.*, **16**, 1 (1897).
15. Cornu, F.: *Jb. Min.*, **1**, 22 (1908).
16. Tertsch, H.: *Cbl. Min.*, 273 (**1917**).
17. Steinmetz, H.: *Zeits. Krist.*, **61**, 380 (1925); Haberlandt, H., and Schiener, A.: *Zeits. Krist.*, **90**, 193 (1935).
18. Schwab, G. M., and Pietsch, E.: *Zeits. phys. Chem.*, **2B**, 262 (1929).
19. Newhouse, W. H.: *Econ. Geol.*, **36**, 622 (1941).
20. Hess, F. L., and Schaller, W. T.: *U. S. Geol. Survey, Bull.* **583**, 30, Pl. XIII (1914).
21. Wild, G. O., and Liesegang, R. E.: *Cbl. Min.*, 737 (**1923**); Brewster, D.: *Trans. Royal Soc. Edinburgh*, **9**, 139 (1823).

22. Chesley, F.: *Am. Mineral.*, **27**, 20 (1942).
23. Headden, W. P.: *Am. Jour. Sci.*, **5**, 314 (1923), *ibid.*, **21**, 301 (1906); see also Brown, W. L., ref. 24.
24. Brown, W. L.: *Univ. Toronto Stud., Geol. Ser.*, no. **35**, 21, Pl. III, Figs. 3, 5 (1933).
25. Doelter, C.: Handb. der Mineralch., Leipzig **4** [3], 228 (1930).
26. Smith, F. G.: *Am. Mineral.*, **27**, 1 (1942).
27. Schneiderhöhn, H., and Ramdohr, P., ref. 9, Fig. 225, among many other descriptions.
28. Luedeking, C., and Wheeler, H. A.: *Am. Jour. Sci.*, **42**, 495 (1891).
29. Nicolson, A. McL.: *Trans. Amer. Inst Elect. Eng.*, 1315, Fig. 7 (**1919**).
30. Ochsenius, C.: *Zeits. Krist.*, **28**, 305 (1897).
31. Stützel, H.: *Cbl. Min.*, 65, (**1937**).
32. Schouten, C.: *Econ. Geol.*, **29**, 611, Figs. 1, 5, 6, 11, 26 (1934).
33. Brammall, A., cited in Grove, A. W., and Mourant, A. E.: *Mineral. Mag.*, **22**, 92 (1929).
34. Liesegang, R. E.: *Naturwiss.*, **3**, 500 (1915).
35. Frondel, C.: *Am. Mineral.*, **19**, 316 (1934); Frondel, C.: *Am. Mus. Nat. Hist.*, Novit., no. **759**, 11 pp. (1934), *ibid.*, no. **695**, 6 pp. (1934), *ibid.*, no. **918**, 4 pp. (1937).
36. Harker, A.: Metamorphism, London, 44 (1939).
37. Becke, F.: *Min. Mitth.*, **6**, 237 (1884).
38. Fackert, H. W.: Inaug. Diss. Albert-Ludwig. Univ., Freiburg, 55 pp., Figs. 20, 22, 29 to 39 (**1929**).
39. Strock, L. W.: Spectrum Anal. with the Carbon Arc Cathode Layer, Adam Hilger, London (1936).
40. Werner, A. G.: Abhandlung von der äusserlichen Kennzeichen der Fossilien, Leipzig, 187 (**1774**).
41. Jameson, R.: System of Mineralogy, Edinburgh, **3**, 355 (1820).
42. Obenauer, K.: *Jb. Min., Beil.-Bd.* **65**, 87 (1932); Kalb, G., and Koch, L.: *Cbl. Min.* 308 (**1929**).
43. Gaubert, P.: *Bull. Soc. Min.*, **25**, 232 (1902).
44. Colomba, L.: *Acc. Lincei Roma, Rend.* **18**, 530 (1909).

DIFFERENTIAL THERMAL ANALYSIS OF CLAY MINERALS AND OTHER HYDROUS MATERIALS.* PART 1.

Ralph E. Grim and Richards A. Rowland†

Abstract

Differential thermal curves are presented for a large number of clay minerals and related silicates. The characteristics of the thermal curves of illites, kaolinites, and montmorillonites, and other clay minerals are discussed. The significance of the thermal data with regard to the lattice structures of the clay minerals, and to the changes they undergo when subjected to heat is considered. On the basis of these considerations certain clay mineral names are discredited.

Thermal curves are presented also for natural and artificial mixtures of clay minerals, and the use of differential thermal curves for identifying clay minerals and estimating their relative abundance in conjunction with *x*-ray, optical, and chemical methods is critically analyzed.

Introduction

The differential thermal method for studying minerals, based on the suggestions made by Le Chatelier (4) in 1887, has been developed and applied with considerable success to the study of clays by several investigators, notably Orcel (24), Cailliere (25), Norton (22), Wohlen (31), and Hendricks and his colleagues (13). Briefly, the method consists of heating a small amount of the substance at a constant rate up to 1000° C. or as close to fusion as is possible experimentally, and recording, by suitable devices, the endothermic and exothermic effects that take place in the material. The temperatures at which the thermal effects take place and their intensities are different for many minerals.

Differential thermal analyses have been published for many of the clay minerals, but unfortunately results of different authors have not always been in agreement. The present paper records additional analyses for many of these minerals and seeks to clarify some of the controversial points. Analyses are presented also for many additional materials that have not been studied heretofore by this method. Explanations are suggested for some of the thermal reactions based on changes that take place in the various minerals.

Apparatus and Analytical Procedure

The differential thermal analyses were made in a furnace consisting of a horizontal tube of alundum 12 inches long and 2 inches inside diameter, wound in the middle with 46 feet of coiled Kanthal A wire and surrounded

* Published with the permission of the Chief, Illinois State Geological Survey, Urbana, Illinois.

† Petrographer and Assistant Petrographer, respectively, Illinois State Geologial Survey, Urbana, Illinois.

with 4 inches of refractory insulating brick. A heating rate of approximately 10°C. per minute was obtained by placing a motor-driven variable transformer in the line.

The specimen holder was a nickel block one inch square and $\frac{5}{8}$ inch deep with four holes each $\frac{1}{4}$ inch in diameter and $\frac{3}{8}$ inch deep, mounted on an alundum cylinder that fit inside the furnace tube. The sample was placed in one of the holes of the specimen holder, and calcined aluminum oxide, which undergoes no thermal reaction up to 1000°C., was placed in the other three holes. A platinum-platinum 10 per cent rhodium thermocouple with the junction in one of the masses of aluminum oxide was attached to a reflecting galvanometer, and the furnace temperature was recorded photographically. A similar thermocouple was placed in another of the masses of aluminum oxide and attached to a potentiometer. The readings from the potentiometer were flashed onto the photographic record in order to evaluate the curve recording the furnace temperature.

A double junction difference thermocouple, consisting of two platinum leads joined by platinum 10 per cent rhodium wire, was placed with one junction in the sample and the other in the remaining mass of aluminum oxide. When the temperature of the sample was greater or less than that of the aluminum oxide, because of a thermal reaction, a potential difference was set up in the thermocouple. The difference thermocouple was attached to a second reflecting galvanometer and the temperature differences were recorded photographically on the same sheet used to record the furnace temperature.

By varying the series resistance in the difference thermocouple circuit, different vertical exaggerations can be obtained for the same temperature difference. Resistances up to 400 ohms were used, and on the diagrams (Figs. 2–14) scale *A* represents 100 ohms and scale *B* represents 200 ohms series resistance. Varying the resistance is important because the magnitude of the thermal reactions is very different for different minerals. Thus, a vertical scale designed for the thermal reactions of kaolinite may fail to show the thermal reactions of the micas because the intensity of the mica thermal reactions is about one-tenth that of kaolinite. In Fig. 1, the vertical scales used in most of the present work are given. By applying these scales to the figures that follow, the temperature difference represented by the peaks of each curve can be determined. The scales were constructed by measuring the swing of the galvanometer for known temperature differences.

All samples were ground to pass a 60-mesh sieve, and an attempt was made to pack each sample the same way in the specimen holder. The weight of the sample used was determined for each run. All of the ground samples, except those containing halloysites, were placed in an oven and

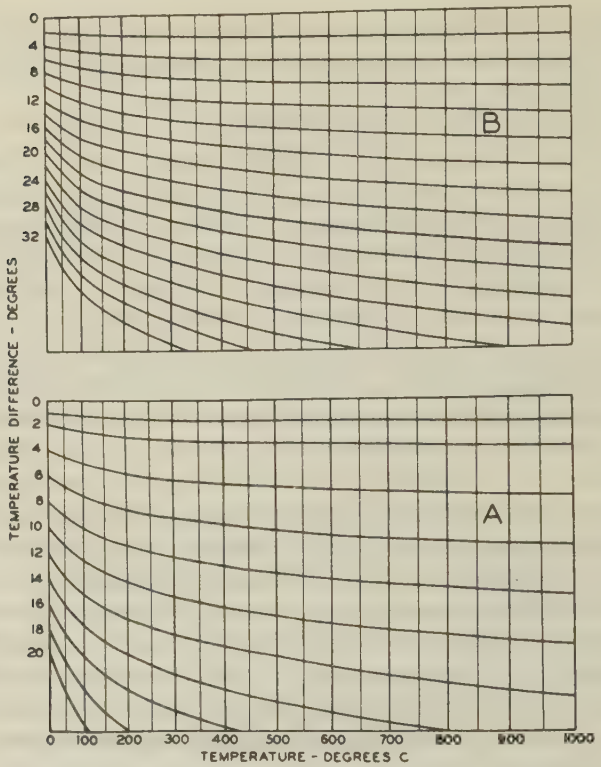

FIG. 1. Scales for determining the temperature differences recorded by the peaks of the thermal curves. Scale *A*—100 ohms series resistance; scale *B*—200 ohms series resistance.

dried at 90°C. for 12 hours and then were placed in a desiccator over a saturated solution of hydrous calcium nitrite ($Ca(NO_2)_2 \cdot 4H_2O$) which gives a relative humidity of 46 per cent at 30°C. (27). Each sample remained in the desiccator at least 24 hours before being placed in the furnace. This procedure was necessary so that the initial part of the analyses representing heat adsorption due to loss of adsorbed water would be comparable. *X*-ray* and optical studies were made of all the samples investigated and chemical analyses were made of many of them.

In order to obtain reproducible results great care was taken to pack all the samples the same way and to keep the positions of the thermocouple junctions constant (18). Since the initial portions of the differential thermal curves vary with slight changes in the rate of heating because

* All *x*-ray analyses were made by Dr. W. F. Bradley of the Illinois State Geological Survey. Dr. Bradley read the manuscript, and offered many helpful suggestions which are hereby gratefully acknowledged.

different room temperatures and humidities alter the starting rate of heating, this range is the least precise. Experience suggests that attempts to estimate quantitatively the mineral components of mixtures can hope for an accuracy of no more than 10 per cent. Experimental difficulties in attaining uniform packing, slight variations in heating rate, etc., prevent greater accuracy. Further, the weight of the sample used must be taken into consideration in qualitative as well as quantitative work.

Experimental Results

Oxides and hydroxides

Quartz shows an endothermic reaction (Fig. 2*A*) at about 565°C. corresponding to the transformation from the α to β form. The curve for quartz was obtained with great vertical magnification, using only 50 ohms resistance. The peak at 565°C. represents a temperature difference of only about 2°C. Some runs with quartz show a slight break in the curve at about 870°C., the transformation point of quartz to tridymite. Since all of the curves obtained for quartz do not show the break at 870°C., its significance is questionable.

Orcel (24) reported that goethite exhibited an endothermic reaction at about 450°C. and limonite at about 350°C. The curves presented here (Fig. 2*B* and *C*) show peaks at about 400°C. and 300°C., respectively. This apparent discrepancy is probably due to differences in the material studied. There are several forms (26, 30) of hydrated ferric iron oxide, and natural samples are apt to be unlike mixtures. The specific hydrates and their forms have not been precisely characterized and further work is necessary before their thermal reactions become well known. The limonite curve was obtained with 400 ohms resistance in the thermocouple circuit, and the goethite curve with only 100 ohms. Even with the increased resistance, the peak for limonite is larger than that for goethite, indicating that the thermal reactions of the various hydrates are of considerably different magnitude.

Gibbsite, according to Norton (22), Orcel (25), and Jourdain (15), shows an endothermic peak at about 350°C. and diaspore, according to Orcel (25) and Norton (22), exhibits an endothermic peak at about 550–575°C. The curves shown in Fig. 2 check these findings. The sample of gibbsite (2*D*) also contains some kaolinite which is responsible for the small endothermic reaction at 550°C. and the exothermic reaction at 950°C. Both curves were obtained with 100 ohms resistance. The endothermic reactions correspond to the dehydration of the minerals. According to Deflandre (6), diaspore upon dehydration develops a structure similar to corundum, and gibbsite, according to Bragg (2), dehydrates to böhmite and this in turn to γ-Al_2O_3, a spinel.

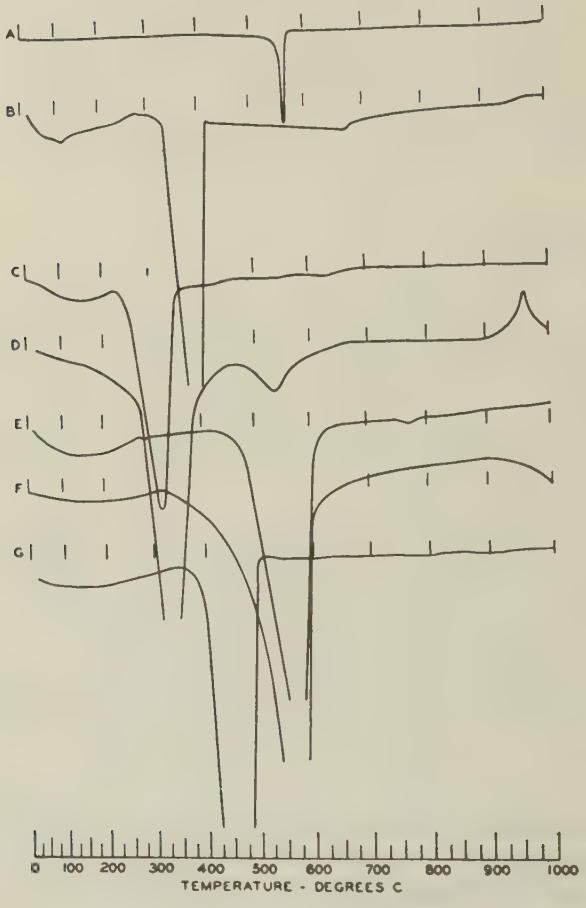

FIG. 2. Oxides and hydroxides.

A. Quartz, Ottawa, Illinois.
B. Goethite, El Paso County, Colorado.
C. Limonite, University of Illinois collections.
D. Gibbsite, Saline County, Arkansas.
E. Diaspore, Chester, Massachusetts.
F. Brucite, Brewster, New York.
G. Brucite, Lancaster, Pennsylvania.

The brucite curve (Fig. 2*G*) obtained with 100 ohms resistance, shows an endothermic reaction at 425–475°C. accompanying dehydration. According to Büssem and Köberich (3) brucite dehydrates to cubic periclase. Sample 2*F*, also listed as brucite, has optical properties like those of hydromagnesite (28), and therefore its differential thermal curve is probably not the characteristic one for brucite.

Kaolinite and halloysite

Many investigators have recorded the endothermic reaction of kaolinite at 550–600°C. as well as the abrupt intense exothermic reaction at 950–1000°C., and these findings are checked by the present work (Figs. 3*A*, *B*, *C*). The endothermic peak accompanies the dehydration of the mineral, and, according to Insley and Ewell (14), the exothermic reaction is associated with the formation of γ-Al_2O_3. Sample 3*B* contains gibbsite in addition to the kaolinite. The explanation for the peculiar initial endothermic peak of 3*A* is not known.

Hydrated halloysite* (halloysite of Mehmel (21), hydrated halloysite of Hendricks (11) shows the same thermal reactions (Fig. 3*F*, *G*) as kaolinite, with an additional sharp endothermic reaction at 100–150°C. accompanying the loss of $2H_2O$ and the transition to halloysite. After heating the mineral in an oven at 90°C. for several hours the initial endothermic peak is almost entirely lost and the curve (Fig. 3*E*) is like that of kaolinite. Attempts to develop the initial endothermic peak in kaolinite or halloysite by rewetting the material that had been dried were unsuccessful (3*D* and 3*E*). Norton (22) has suggested that halloysites show an additional endothermic peak at about 325°C. and that the endothermic peak between 500°C. and 600°C. takes place at slightly lower temperatures for halloysites than for kaolinite. These suggestions could not be checked, and the peak at 325°C. may represent some gibbsite in Norton's material.

The differential thermal curves present no evidence that halloysite differs from kaolinite, or that hydrated halloysite differs from kaolinite, except by the presence of the initial endothermic peaks representing water lost at low energy levels. Loss of the swelling water from montmorillonite yields an endothermic reaction in the same low temperature region.

* In the present paper the halloysite minerals are designated according to the nomenclature suggested by Hendricks (11), i.e., the form with the composition $Al_2O_3 \cdot 2SiO_2 \cdot 4H_2O$ is designated hydrated halloysite, and the form $Al_2O_3 \cdot 2SiO_2 \cdot 2H_2O$ is designated halloysite. The expression "a halloysite" is used when the particular form cannot be identified.

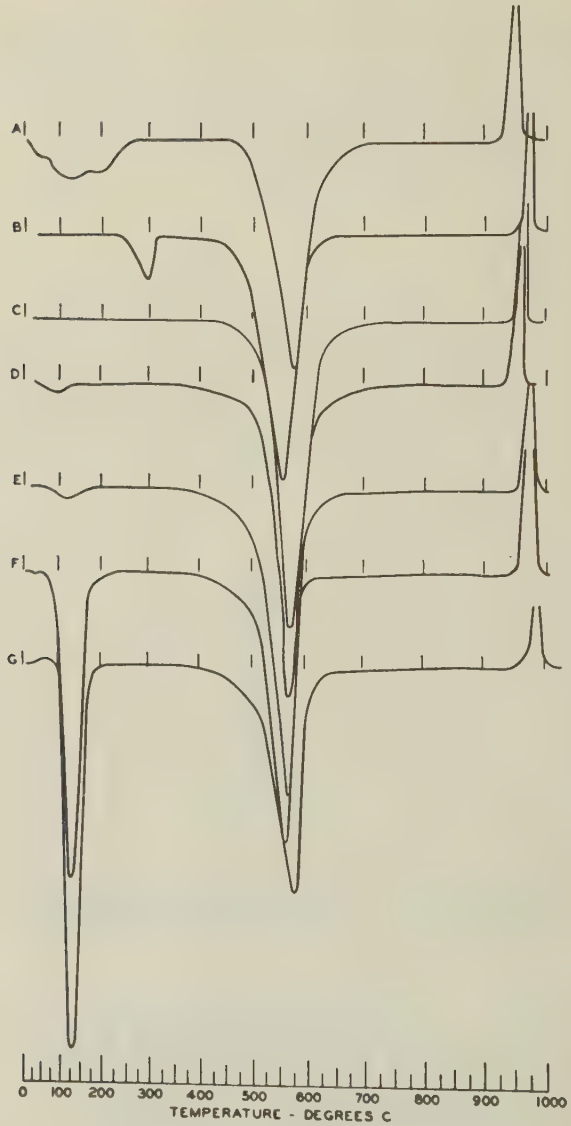

FIG. 3. Kaolinites and halloysites. Scale *B*.

A. Kaolinite, Anna, Illinois.
B. Kaolinite, Spruce Pine, North Carolina.
C. Kaolinite, Dry Branch, Georgia.
D. Kaolinite, wetted and then dried at room temperature, Dry Branch, Georgia.
E. Halloysite, dried at 90°C., wetted, and then redried at room temperature, Djebel Debar, Algeria, from U. Hofmann, University of Rostock, Rostock, Germany.
F. Hydrated halloysite, Eureka, Utah.
G. Hydrated halloysite, Djebel Debar, Algeria.

Illites

Illites (Fig. 4) show endothermic peaks at 100–200°C., 500–650°C., and about 900°C., and an exothermic peak immediately following the third endothermic peak. The exothermic peak is not always very pronounced (Fig. 4*A*, *B*, *C*) and occurs in some materials slightly above the highest temperature (1000°C.) of most of the experiments. The endothermic peak at 500–650°C. accompanies the loss of most of the water

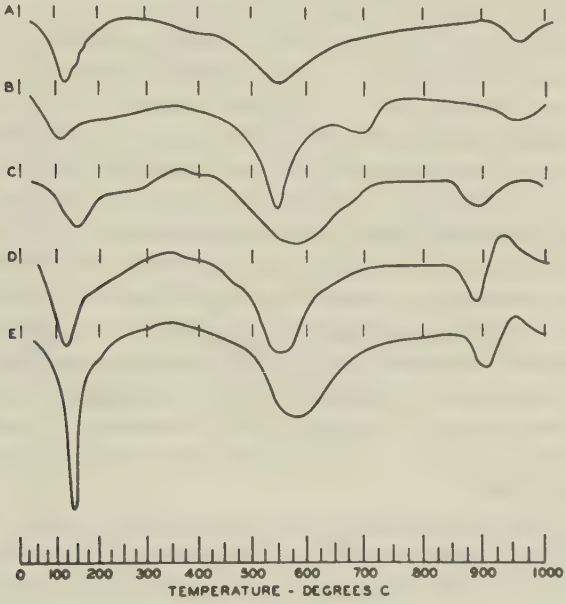

FIG. 4. Illites. Scale *A*.

A. Glauconite, University of Illinois collections.
B. "Glimmerton," Sarospatak, Hungary, from U. Hofmann, University of Rostock, Rostock, Germany.
C. Illite, purified from shale, Alexander County, Illinois.
D. Illite, purified from underclay, Vermilion County, Illinois.
E. Illite, purified from underclay, Grundy County, Illinois.

from the lattice, and the third endothermic peak is interpreted as being associated with the final destruction of the illite structure. This is in accordance with the finding of Grim and Bradley (9) that the illite lattice is not destroyed when most of the water is lost from the lattice and that the breakdown of the structure comes at a higher temperature followed by the formation of spinel. The exothermic reaction following the third endothermic peak is probably associated with the formation of spinel.

The halloysites, kaolinite, and the illites all show an endothermic reaction between 500°C. and 650°C., but the reaction in kaolinite and the halloysites is sharper and has about ten times the intensity of the reaction in the illites. Because of this difference in reaction intensity the resistance in the galvanometer circuit must be varied for the different clay minerals. If the apparatus is set up to record a moderate galvanometer swing for the reactions in kaolinite, the reactions of illites may well go undetected. Perhaps this explains why several previous workers have failed to detect the characteristic thermal reactions of the illites.

The reason for the greater intensity of the endothermic reaction in the two-layer kaolinite-type lattice between 500°C. and 650°C. than in the three-layer mica-type lattice at the same temperature is not entirely clear. A partial explanation is that the reaction represents the loss of more water from the two-layer lattices than from the three-layer lattices, and that the reaction represents also destruction of the two-layer lattice, whereas the three-layer lattice is not destroyed until a higher temperature is reached and in a separate reaction. These facts, however, do not seem entirely adequate to account for the difference in intensity.

The illite curves are less regular and show more variation than the kaolinite curves. This is expected as illite represents a group of minerals and is not a specific mineral name. The final exothermic reaction is particularly variable, and frequently (see discussion of montmorillonite curves) takes place at a temperature above that usually attained in the furnace, i.e., 1000°C.

Sample 4*B* is representative of the type of clay mineral described by Maegdefrau and Hofmann (20) as "glimmerton" (mica-clay mineral). The thermal curve for sample 4*B* is like that of the illites with an additional endothermic peak at about 700°C. indicating that montmorillonite is also present.

The curve for the glauconite (4*A*) is quite like that of the illites. Additional glauconite samples must be studied before the significance of this similarity can be fully interpreted.

Montmorillonites

All of the montmorillonite samples represented by differential thermal curves in Fig. 5 yielded clear *x*-ray diffraction patterns showing the distinct lattice expansion characteristic of the mineral. The curves show an initial endothermic peak at 100–250°C., apparently representing the loss of water held between the basal planes of the lattice structure (i.e., swelling water). Hendricks et al. (13) have mentioned the dual character frequently shown by this montmorillonite peak and discussed its relation to the exchangeable base composition of the mineral. This initial peak

is larger and extends over a wider temperature range than the similar peak for illites, and it extends over a much wider temperature range than the initial peak for hydrated halloysite. The presence of this initial endo-

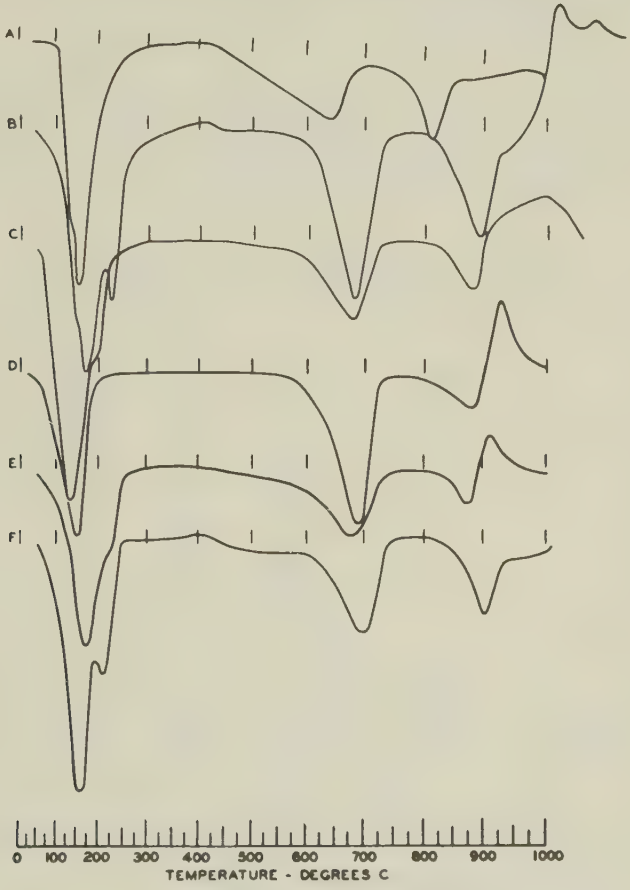

FIG. 5. Montmorillonites. Scale *A*.

A. Otay, California.
B. Rideout, Utah.
C. Geisenheim, Germany, from K. Endell, Technische Hochschule, Berlin, Germany.
D. Upton, Wyoming.
E. Aberdeen, Mississippi.
F. Tatatila, Vera Cruz, Mexico, U. S. Nat. Mus. 101, 836.

thermic peak in these three clay minerals suggests that they all possess water other than pore water (which causes no thermal reaction above 100°C.) and lattice water (which is lost at a higher temperature). Studies

(12, 8) of the water relationships in montmorillonite suggest that this water is held on the basal planes of the unit cells and further that the water itself has distinctive properties. Such water would correspond to the "planar water" postulated by Kelley and his colleagues (16). It follows that other clay minerals, e.g., illites, can have some of this type of water without also having expanding lattice characteristics.

Montmorillonite yields a second endothermic peak between 600°C. and 700°C. corresponding to the loss of lattice water. The explanation for the slightly lower temperatures of the second and third endothermic peaks of the Otay sample (Fig. 5*A*) is not known.

Table 1. Chemical Analyses of Montmorillonite

	5A	*5B*	*5D*	*5E*	*5F*
SiO_2	50.30	66.02	64.32	64.17	52.09
Al_2O_3	15.96	19.97	20.74	17.14	18.98
Fe_2O_3	.86	.71	3.03	4.81	.06
FeO		.13	.46		
MgO	6.53	5.04	2.30	3.90	3.80
CaO	1.24	1.97	.52	1.48	3.28
Na_2O	1.19	.12	2.59	.21	
K_2O	.45	.09	.39	.48	
TiO_2		.19	.14		
Ign. loss		6.51			
Total		100.75			
H_2O+	23.61	6.42	5.15	7.78	7.46
H_2O-		11.89			14.75
SiO_2/R_2O_3	5.12	5.15	4.83	5.40	5.05
SiO_2/Al_2O_3	5.34	5.63	5.28	6.36	5.20

5*A* Otay, California. *Jour. Am. Cer. Soc.* **9**, 88 (1926).

5*B* Rideout, Utah, Analysis made under the supervision of O. W. Rees, Ill. State Geol. Survey.

5*D* Upton, Wyoming, American Colloid Co. (1940).

5*E* Aberdeen, Mississippi, American Colloid Co. (1940).

5*F* Tatatila, Vera Cruz, Mexico, Analysis from W. F. Foshag, U. S. Nat. Museum.

There is no satisfactory explanation of why the second endothermic reaction corresponding to the loss of lattice water takes place about 100°C. higher in montmorillonite than in the illites. Both of them have three-layer lattices and about the same amount of lattice water, yet the one which is found in larger and more perfectly crystalline masses (8) and does not expand, i.e., the illites, loses most of its lattice water at the lower temperature.

Montmorillonite shows a third endothermic peak at about 900°C. corresponding to the final breakdown of the montmorillonite lattice. Grim and Bradley (9) have shown that this clay mineral, like illites, first loses most of its lattice water, and later at a higher temperature the structure is destroyed. This third endothermic peak appears to be characteristic of three-layer clay minerals since it is not shown by kaolinite and the halloysites.

The third endothermic reaction is followed by an exothermic effect probably accompanying the formation of spinel (9). A comparison of this peak with the chemical analyses given in Table 1 shows that this exothermic reaction takes place at a slightly lower temperature in samples 5*D* and 5*E* which have the highest iron content. Additional data support the conclusion that the exothermic reaction is closely related to the iron content. Samples with low iron content show the exothermic reaction above 1000°C. and hence it is not recorded unless the temperature is carried above 1000°C. (5*B*).

Previous workers (15, 22, 24, 25) have recorded that montmorillonite curves show three endothermic peaks, but except for the initial one, somewhat different temperatures for the reactions were recorded. The final exothermic reaction does not seem to have been detected before.

Miscellaneous clays containing montmorillonite

Differential thermal curves are shown in Fig. 6 for a miscellaneous group of samples known to contain montmorillonite. Curves 6*A* and 6*F* are like those of montmorillonite except that 6*F* contains additional material, probably brucite, which is responsible for the 500°C. endothermic peak. These samples (6*A* and 6*F*) yield excellent diffraction patterns of montmorillonite, and their accurately measurable optical properties are also those of montmorillonite. Sample 6*A* was heated to 1100°C. to confirm the presence of the final exothermic peak above 1000°C. in samples with low iron content.

Samples 6*C*, 6*D*, and 6*E* of Fig. 6 yield curves with endothermic peaks between 500°C. and 600°C. and also between 600°C. and 700°C. The latter peak indicates that these samples contain montmorillonite and the former peak shows the presence of some other clay mineral. Illites, kaolinite and the halloysites all give endothermic reactions between 500°C. and 600°C. The characteristics of the third endothermic peak and the final exothermic peak are more like those of the illites than those of kaolinites or the halloysites. The suggested interpretation of the curves is that these samples are mixtures of montmorillonite and illite, using illite, as originally defined (10), as a general term for clay minerals closely related to the micas.

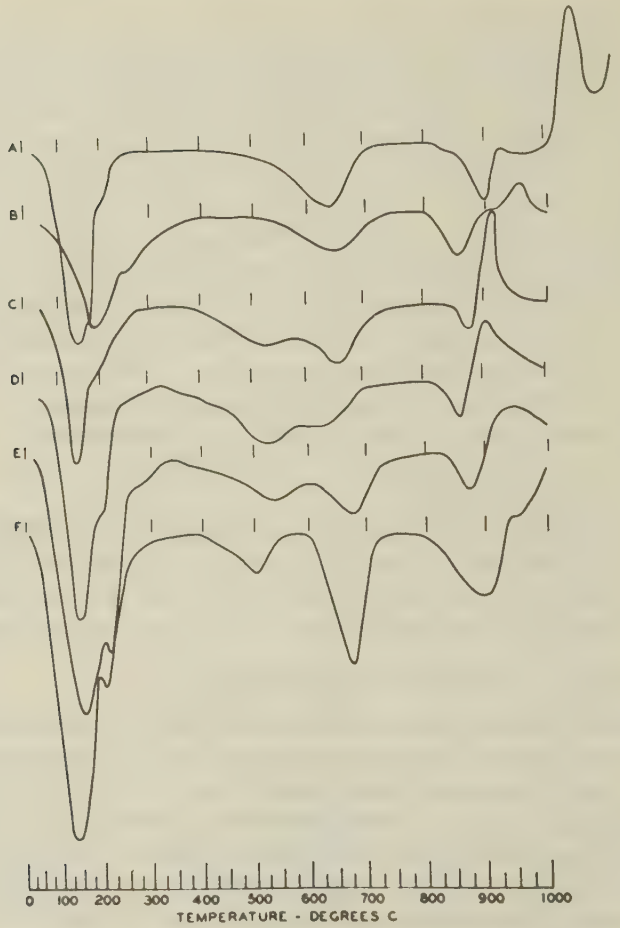

FIG. 6. Miscellaneous clays containing montmorillonite, Scale *A*.

A. Acid activated bentonite, Jackson, Mississippi.
B. Metabentonite, High Bridge, Kentucky.
C. Bentonite, Saline County, Arkansas.
D. Bentonite, Pontotoc County, Mississippi.
E. Bentonite, Phillips County, Kansas.
F. "Montmorillonite," San Bernadino County, California.

X-ray diffraction analyses of samples 6*C*, 6*D*, and 6*E* yielded very poor patterns that are in accord with the interpretation that these samples are composed of more than one clay mineral. The presence of montmorillonite is shown definitely by the patterns, but other constituents cannot be identified. The optical values of the samples cannot be determined accurately—only a mean index of refraction and a suggestion

that the birefringence is moderately high. The character of the birefringence is in accord with the interpretation that illite rather than kaolinite or a halloysite is mixed with the montmorillonite.

TABLE 2. CHEMICAL ANALYSES OF MISCELLANEOUS CLAYS CONTAINING MONTMORILLONITE

	6*A*	6*C*	6*D*	6*E*
SiO_2	66.69	59.87	57.55	57.54
Al_2O_3	19.67	21.70	19.93	20.23
Fe_2O_3	1.01	6.86	6.35	5.60
FeO		.17	.95	.24
MgO	4.66	2.89	3.92	3.29
CaO	1.00	.95	1.94	2.92
Na_2O		.09	.33	.89
K_2O		.14	.59	2.10
TiO_2		.27	.32	.66
Ign. loss	7.14	7.74	8.53	7.08
Total	100.17	100.68	100.41	100.55
H_2O+		7.53	8.51	6.93
H_2O-	10.73	6.07	7.43	5.51
SiO_2/R_2O_3	5.58	3.90	4.10	4.12
SiO_2/Al_2O_3	5.76	4.68	4.92	4.84

Analyses made under the supervision of O. W. Rees, Ill. State Geol. Survey.
6*A* Acid-activated bentonite, Jackson, Mississippi.
6*C* Bentonite, Saline County, Arkansas.
6*D* Bentonite, Pontotoc County, Mississippi.
6*E* Bentonite, Phillips County, Kansas.

Chemical analyses (Table 2) of samples 6*C*, 6*D*, and 6*E* show that the K_2O content of 6*C* and 6*D* is lower than would be anticipated if illite is the additional clay mineral. However, the potash content of illites is variable, and the chemical data are not believed to be strong evidence against the presence of illite. Except for the low K_2O content, the chemical data are in accord with the illite interpretation. In addition to clay minerals, these samples contain some hydrated ferric iron oxide which may account for the rise in the thermal curves between 400°C. and 500°C.

The differential thermal curve for the metabentonite sample (Fig. 6*B*) is like that of montmorillonite except that the second endothermic peak is less abrupt. However, the *x*-ray pattern of the material is similar to that of micas, and is particularly like the pattern for glauconite. The reason for the apparent conflict between the thermal and *x*-ray data is not clear, and the optical properties cannot be measured with sufficient accuracy to offer additional evidence. This is the only sample of clay studied so far in which an endothermic peak between 600°C. and 700°C.

did not indicate an expanding lattice mineral. It is further evidence, if any is needed, of the danger of identifying the constituents of a clay material on the basis of a single set of characteristics, whether they be thermal, optical, x-ray, or any other one.

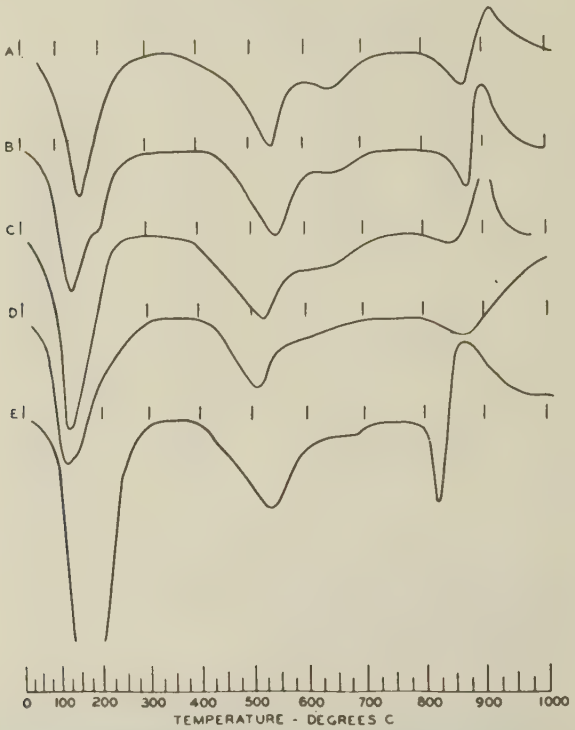

FIG. 7. Miscellaneous clays containing montmorillonite, Scale A.

A. Fuller's earth, Twiggs County, Georgia.
B. Bentonite, Harris County, Texas.
C. Bentonite, Ouachita Parish, Louisiana.
D. "Montmorillonite," Glen Riddle, Pennsylvania, U. S. Nat. Mus. 103058
E. "Montmorillonite," Sierra de Guadalupe, Atzcapozalco, Mexico, U. S. Nat. Mus. 7591.

Differential thermal curves for an additional set of samples thought to contain montmorillonite are presented in Fig. 7. All the curves show a large endothermic peak at 500–600°C. and a smaller one between 600°C. and 700°C. The small peak indicates the presence of some montmorillonite, but the larger peak between 500°C. and 600°C. suggests that the principal constituent is either kaolinite, a halloysite, or illite. The character of the third endothermic peak and the final exothermic peak of samples 7A, 7B, 7D, and 7E suggests illite whereas this part of the curve for sample 7C suggests kaolinite or a halloysite.

X-ray patterns of all samples represented in Fig. 7 were poor and all that can be determined from them is that the samples contain a small amount of montmorillonite. Only a mean index of refraction can be determined for these samples. All of them except sample 7*C* appear to have a moderately high birefringence which is in accord with the suggestion that kaolinite or a halloysite is present in 7*C* whereas an illite is present in the other samples. Chemical analyses for most of these samples are given in Table 3, and as noted in discussing the previous group of samples the low K_2O content of the materials is not necessarily evidence against the illite interpretation.

Table 3. Chemical Analyses of Miscellaneous Clays Containing Montmorillonite

	7*A*	7*B*	7*C*	7*E*
SiO_2	62.91	60.13	56.99	50.44
Al_2O_3	19.47	21.57	22.70	16.26
Fe_2O_3	4.84	5.42	9.27	5.38
FeO	.22	.15	.31	
MgO	3.18	2.67	1.65	3.92
CaO	.25	1.58	.61	.72
Na_2O	.04	.38	.25	
K_2O	.63	1.02	.21	
TiO_2	.58	.64	.38	.42
Ign. loss	8.20	7.00	8.29	
Total	100.32	100.56	100.66	
H_2O+	7.97	6.76	8.07	6.30
H_2O-	5.66	6.56	5.77	16.00
SiO_2/R_2O_3	4.74	4.07	3.88	4.33
SiO_2/Al_2O_3	5.44	4.73	4.26	5.25

Analyses 7*A–C* made under the supervision of O. W. Rees, Ill. State Geol. Survey.

7*A* Fuller's earth, Twiggs County, Georgia.

7*B* Bentonite, Harris County, Texas.

7*C* Bentonite, Ouachita Parish, Louisiana.

7*E* "Montmorillonite," Sierra de Guadalupe, Atzcapozalco, Mexico. Analyses from W. F. Foshag, U. S. Nat. Museum.

The data here presented suggest that many bentonites and other materials previously thought to be composed entirely of montmorillonite, contain large and frequently dominant amounts of other clay minerals. Orcel (24) has noted the presence of kaolinite in some bentonites, but the fact that clay minerals other than montmorillonite are the dominant constituents in some of them has not been recorded. The evidence suggests that this other constituent is usually an illite, but that in some samples it may be kaolinite or a halloysite.

(*To be continued*)

AMERICAN SYNTHETIC EMERALD*

Austin F. Rogers, *Stanford University*
and
Francis J. Sperisen, *San Francisco, California.*

Abstract

The synthetic emerald here described has been made by Carroll F. Chatham, San Francisco, although the method of manufacture cannot be disclosed at present. Cut stones made of the material are small but of very good quality.

The emerald crystals are short prismatic in habit, and in color are comparable to good Colombian emeralds. The chemical analysis shows silica, alumina, beryllia, some chromium oxide, small amounts of alkalies, and small amounts of other constituents.

Optical tests prove that the crystals are emerald. They are slightly pleochroic and show certain optical anomalies.

The synthetic emerald is distinguished from natural emerald by the character of the inclusions.

The first successful synthesis of emerald was that of Hautefeuille and Perrey (1) in France in 1888. Through the courtesy of Dr. J. Orcel, curator of the Muséum National D'Histoire Naturelle of Paris, a small vial of these emeralds was obtained. They are prismatic in habit with the forms $\{10\bar{1}0\}$, $\{0001\}$, and occasionally $\{h0\bar{h}l\}$, and are about 1 mm. long. They have a good emerald green color.

More recently synthetic emerald has been produced in the laboratories of the Interesse Gemeinschaft Farbenindustrie Aktiengesellschaft in Bitterfeld, Germany. This emerald is known as "Igmerald." It was first announced in 1930. A number of papers on the synthetic emerald of the I. G. Farbenindustrie have appeared in the last decade; the most complete one is that of E. Schiebold (2) of the University of Leipzig.

Synthetic Emerald in the United States

The first synthetic emerald produced in the United States was made by Mr. Carroll F. Chatham (3), chemist of San Francisco. Colorless beryl was made by Mr. Chatham as early as 1930. In 1935 he succeeded in making the first emerald crystals of appreciable size (one carat in the rough). Unfortunately the method of producing the emerald cannot be divulged.

A number of different lots of the synthetic emeralds have been submitted to us for study by Mr. Chatham.

Preliminary tests by one of us (F.J.S.) in September, 1940, proved that the specimens were emeralds and the conclusion was also reached that they were synthetic. The articles by Anderson and Payne (4) of the London Gem-testing Laboratory, and by Foshag (5) of the U. S. Na-

* Paper presented at the twenty-second annual meeting of the Mineralogical Society of America, Boston, December 29, 1941.

tional Museum were of considerable aid in this examination. Since then the preliminary results have been confirmed by more complete tests.

One lot of the synthetic emeralds consists of small (about 1.3 mm. long) slender, well-developed, prismatic crystals with the forms $\{10\bar{1}0\}$, $\{11\bar{2}0\}$, $\{0001\}$, and occasionally $\{h0\bar{h}l\}$. They are slightly pleochroic

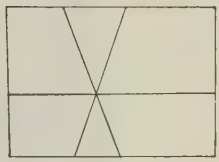

FIG. 1 (×25). Synthetic emerald crystals.
FIG. 2. Vicinal faces replacing the first order prism on synthetic emerald.

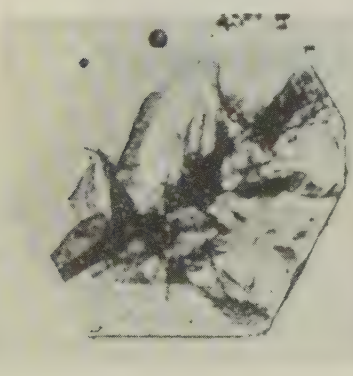

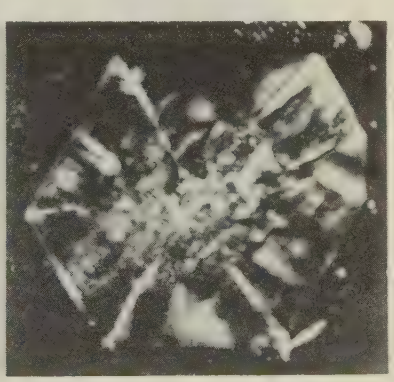

FIG. 3 (×45). Basal section of synthetic emerald showing growth stages and characteristic inclusions.
FIG. 4. (×45). The same section between crossed nicols showing birefringent areas.

from blue-green (α) to yellow-green (γ), have parallel extinction and are length-fast. Groups of these crystals furnish excellent specimens for micro-mounts. Associated with the emerald are a few colorless crystals which are identified as phenacite (Be_2SiO_4) by indices of refraction and crystal habit (forms: $\{11\bar{2}0\}$ and $\{10\bar{1}1\}$).

The main lot of synthetic emerald used in this study consists of crustiform aggregates with euhedral crystals on the free surface. The individual crystals are short prismatic in habit and measure from 2.5 to 5 mm. in longest dimension. The forms are {0001}, $\{10\bar{1}0\}$, and $\{11\bar{2}0\}$. On some of the crystals ill-defined vicinal faces take the place of faces of the first order prism. The vicinal forms present are a steep hexagonal dipyramid and a dihexagonal dipyramid as shown in the sketch of Fig. 2.

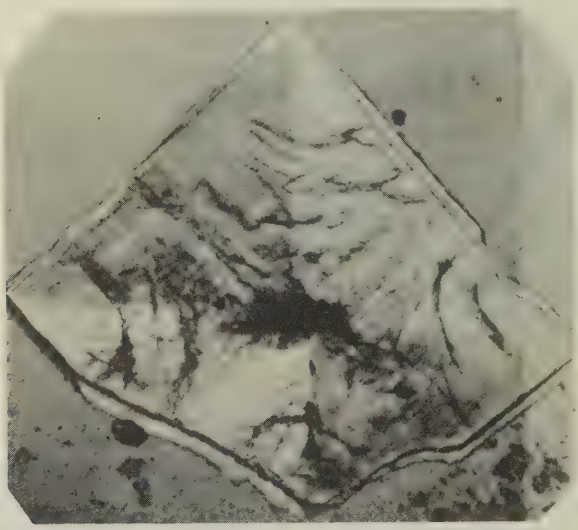

FIG. 5. (×50). Longitudinal section of synthetic emerald between crossed nicols with superimposed quartz wedge.

Sections of the synthetic emeralds about 0.2 mm. thick were skilfully prepared by Mr. Alexander Tihonravov. Photomicrographs of some of these are shown in Figs. 3–6. A basal section bounded by $\{10\bar{1}0\}$ and three faces of the $\{11\bar{2}0\}$ form shows a prominent zonal structure due to a slight color difference in the growth stages (Fig. 3). Between crossed nicols portions of this section exhibit appreciable birefringence which is well brought out in Fig. 4. Thin birefringent strips divide the section into sectors. The main portion of the section is uniaxial with a negative sign.

Optical anomalies are also shown in longitudinal sections such as Fig. 5, which was taken between crossed nicols with a quartz wedge to bring out contrast in the sectors. Here the *c*-axis of the crystal is parallel to the NE-SW direction which means that the habit is thick tabular. The longitudinal sections are pleochroic with α = bluish green and γ = yellow green.

Indices of Refraction

The indices of refraction of the synthetic emerald determined by the prism method on a cut prism of about 60° angle in sodium light are:

$$n_\alpha = 1.573,\ n_\gamma = 1.578;\ n_\gamma - n_\alpha = 0.005.$$

The indices are a little higher than those recorded for the I. G. Farbenindustrie synthetic emerald, but are very similar to indices of the Russian emeralds from the Urals.

Specific Gravity

The specific gravity of about 0.3 g. of carefully selected fragments of the synthetic emerald free from visible impurities determined with a small pyknometer was found to be 2.667.

Inclusions

Inclusions in precious stones are especially important since the inclusions in synthetic stones and natural stones each have their distinctive features. The inclusions present in the Chatham synthetic emeralds are of two kinds: (1) clusters of dark red equant isotropic crystals, ca. 0.01 mm. in size with high relief, which have not been identified, and (2) curved sheets, wisps, or "curtains" of liquid-gas inclusions from 0.003 to 0.015 mm. in size and often elongate. Both kinds of inclusions are shown in Fig. 6, the dark red crystals on the right and the "curtains"

Fig. 6 (×60). Inclusions in basal section of synthetic emerald.

near the center of the section. Under higher magnification the liquid-gas inclusions appear as in Fig. 7. The "curtain" is oblique to the section and only a central strip of it is in focus.

FIG. 7 (×200). Liquid-gas inclusions in synthetic emerald.

For comparison, the inclusions of natural emerald from Colombia have also been studied. The specimens were obtained in Colombia by Mr. Basil Prescott some years ago. Fig. 8 shows a general view of the inclu-

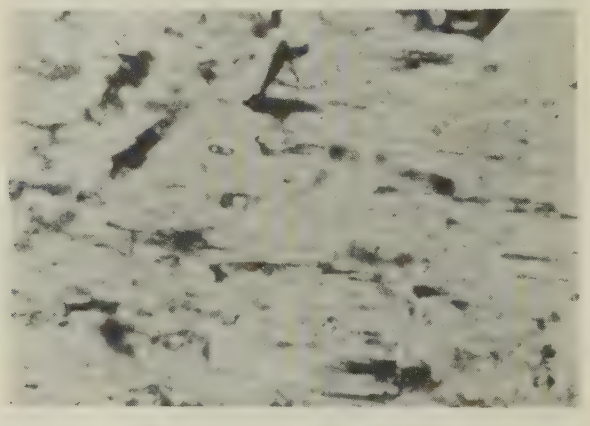

FIG. 8 (×100). Inclusions (negative crystals) in longitudinal section of natural Colombian emerald.

sions which are parallel to the *c*-axis. The dark areas are cavities on the surface of the section which are filled with fine abrasive. Most of the inclusions seem to be negative crystals and these inclusions probably give

a sheen to the cut emerald. A higher magnification of some of the inclusions in the natural emerald shows a liquid with gas bubble and an euhedral cubic crystal of isotropic halite as exhibited in Fig. 9. These inclusions are often flask-shaped. Halite inclusions are apparently characteristic of the Colombian emerald for they have been noted by H. Michel (6).

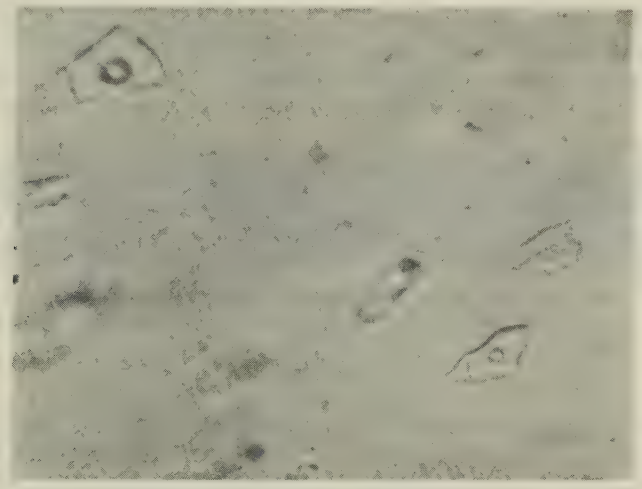

FIG. 9 (×400). Liquid-gas-halite inclusions in natural Colombian emerald.

CHEMICAL ANALYSIS

A chemical analysis of the dark green synthetic emerald made for Mr. Chatham by Curtis and Tompkins of San Francisco gave the following results:

CHEMICAL ANALYSIS OF SYNTHETIC EMERALD BY CURTIS AND TOMPKINS

SiO_2	64.30
Al_2O_3	18.65
BeO	13.20
Fe_2O_3	0.30
Cr_2O_3	2.00
CaO	0.73
MgO	0.10
K_2O	0.21
Na_2O	0.56
H_2O	0.14
TiO_2	0.05
Total	100.24

The emerald green color is evidently due to the chromium content.

Spectrographic Analysis

A spectrographic analysis of the synthetic emerald made in the ultraviolet region by my assistant, Mr. Reynolds M. Denning, showed prominent lines for aluminum, beryllium, and silicon, fair lines for chromium, magnesium, and titanium, and weak lines for calcium, copper, and sodium. The spectrum for the synthetic emerald is reproduced in the central strip of Fig. 10. The spectrogram identifies the specimen as emerald without any doubt. The upper strip of Fig. 10 is the spectrum for the Colombian emerald. The lower strip of the figure is the standard iron ("Armco") spectrum for comparison.

Fig. 10. Spectrograms of natural Colombian emerald (upper strip), synthetic emerald (central strip) and "Armco" iron (lower strip).

Conclusion

Physical and chemical tests of the synthetic emerald produced by Mr. Carroll F. Chatham of San Francisco prove its identity with emerald. It is emerald of good quality which approaches the attractive color of the better grades of Colombian emeralds. This synthetic emerald may be distinguished from natural emerald by the character of its inclusions.

References

1. Hautefeuille, P., and Perrey, A., *Comptes Rendus des Séances de l'Académie des Sciences*, **106**, 1800 (1888).
2. Schiebold, E., *Zeits. Kryst.*, **92**, 435–473 (1935).
3. Personal communication, July, 1942.
4. Anderson, B. W., and Payne, C. J., *Goldsmith's Journal and Gemmologist*, **37**, 407–410 (1938).
5. Foshag, W. F., *Jeweler's Circular-Keystone*, **104**, 73, 75, 91 (1938).
6. Michel, H., *The Pocket-Book for Jewelers*, Part II, Plate XXIIb, G. L. Herz, New York and Vienna. (No date).

MINOR CHEMICAL ELEMENTS IN FLUORITES FROM JAMESTOWN, COLORADO

JOSEPH M. BRAY, *Lafayette College, Easton, Pennsylvania.*

ABSTRACT

Four fluorites from Jamestown, Colorado, were analyzed spectrographically, and twenty minor elements were found to be present. Seventeen others were absent in all samples. Correlation between the minor elements present and the geologic environments of the fluorites was possible. No correlation was possible between minor elements present and radioactivity, fluorescence, or type of wallrock. The most abundant of the minor elements were Sr, Ba, Fe, Y, Cu, Mg, Al, and Si. These probably substitute for Ca in the ionic fluorite structure. The oldest fluorite was the most impure and the youngest was the purest.

INTRODUCTION

The spectrographic investigation upon which this paper is based was performed during 1940 in the Cabot Spectrographic Laboratory of the Geology Department at the Massachusetts Institute of Technology. The primary purpose of the work was to determine what minor chemical elements were present in the fluorites from four different mines in the Jamestown district, and to attempt to correlate the results with actual field relations, as well as with previous similar studies carried out by the writer (Bray, 1942 *a*; 1942 *b*) on the igneous rocks of the region.

The writer wishes to express his deep appreciation to Dr. E. N. Goddard, of the United States Geological Survey, for his invaluable assistance and interest in the problem, and for his suggestions in regard to securing samples. Professor W. H. Newhouse kindly permitted the use of the facilities of the Cabot Spectrographic Laboratory for the analytical work.

GENERAL GEOLOGY OF THE DISTRICT

The Jamestown district is located in Boulder County, Colorado, 10 miles northwest of Boulder, 35 miles northwest of Denver, at the northeast extremity of the Front Range mineral belt. The country rock is composed of pre-Cambrian gneisses and schists intruded by pre-Cambrian granites and a series of Tertiary stocks and dikes ranging from diabase to alaskite. The geology of the Front Range has been discussed by Ball (1908) and by Lovering (1929). Fenneman (1905) has considered the geology of the Boulder area. More recently Goddard (1935) has made detailed studies of the geology and ore deposits of the Jamestown region. Figure 1 is a sketch map (based on the work of Lovering and Goddard, 1938 and 1939) giving the areal geology of the section, together with the locations of the samples used.

The fluorite deposits are genetically related to a granite-quartz monzonite stock, one of the latest of the Tertiary intrusive porphyries. For a complete description the reader is referred to the paper by Goddard (op. cit.)

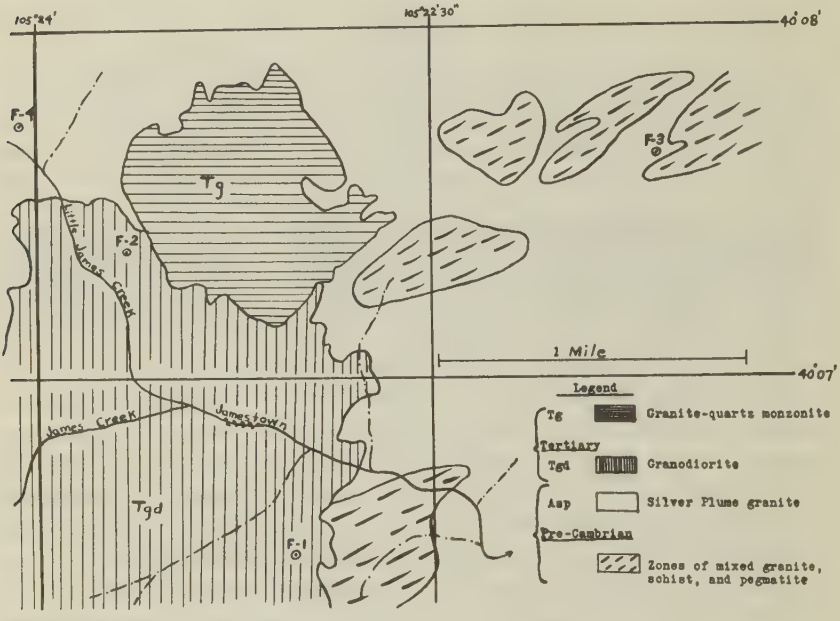

FIG. 1. Geological sketch map of the Jamestown area, showing locations of samples.

The writer (Bray, 1942 *a*; 1942 *b*) has discussed the distribution and relationships of the minor chemical elements in the igneous rocks of the Jamestown district.

THE FLUORITE DEPOSITS

Goddard (op. cit., p. 377) describes the deposits as breccia zones or veins containing a breccia matrix and filling of purple fluorite. Some pyrite, galena, chalcopyrite and coarse-grained quartz are also present. Many fluorite zones appear to be parts of larger barren breccia zones. Other mineral deposits in the district (all younger than the fluorite deposits) are lead-silver veins, pyritic-gold veins, and gold-telluride veins, in order of decreasing age. The oldest mineral deposits tend to be closest to the granite-quartz monzonite stock.

Specimens from the Argo, Brown Spar, Blue Jay and Caledonia mines (see Fig. 1 for locations) were analyzed. The Argo mine is in a fluorite-breccia zone near the parent stock. In this mine fragments of argentifer-

ous galena and gray copper, sphalerite and pyrite are earlier than the fluorite, which is associated with small amounts of pyrite, galena, sphalerite and chalcopyrite. Goddard* reports a speck of pitchblende present in one of his fluorite specimens.

In the Brown Spar mine, which is also in a breccia zone, small quantities of galena, pyrite, and sphalerite are associated with the fluorspar. In the Blue Jay mine, a fluorite vein south of the parent stock and farther from it (and therefore younger?) than the Argo and Brown Spar breccia zones, minor galena, pyrite, and sphalerite are present with the fluorspar. Goddard reports occasional specks of pitchblende. The Caledonia mine is in a pyritic-gold vein, and therefore the mineralization is the youngest.

The relative ages can be tentatively summed up as follows: The Argo and Brown Spar breccia zones are nearest the parent stock and probably are oldest, the Blue Jay fluorite vein is probably intermediate, and the Caledonia pyritic-gold mineralization the youngest.

The Argo and Caledonia deposits are in a wallrock of pre-Cambrian Silver Plume granite, which is medium to coarse in texture, and contains numerous lath-like orthoclase phenocrysts in a groundmass of quartz, oligoclase, biotite and muscovite. The Blue Jay and Brown Spar deposits are in a wallrock of Tertiary granodiorite, which is medium in texture, and contains very abundant hornblende, andesine-labradorite, orthoclase, and less quartz, sphene and magnetite.

The Analyses

Analytical Procedure

The analytical work was performed with a 21-foot, 30,000-line (per inch concave) grating spectrograph on a Wadsworth mounting. The particular method used was the cathode-layer carbon arc technique described by Strock (1936), with special modifications described by the writer (1942 *a*).

Results

Table 1 lists the four analyses and other pertinent data, including explanation of the symbols used. The quantities as expressed are spectrographic, and should be considered only as such. The symbols should be used only in comparing the quantities of a single element in the several samples. Comparisons between amounts of the several elements in a single sample should be made with extreme care, if at all, because the spectrographic sensitivities of the different elements vary greatly, and "large" for one might actually be less in percentage than a quantity designated as "medium" for an element spectrographically more sensitive.

* Personal communication.

TABLE 1. SPECTROGRAPHIC ANALYSES OF THE FLUORITES

Sample	Na	K	Mg	Sr	Ba	Al	Sc	Y	La	Ce	Nd	V	Cr	Mn	Fe	Pb	Ag	Si	Cu	Be
F-4	M	S	M	VL	VL+	L−	T	M+	L	T	T	M−	T	S+	L	S+	A	VL	M	T
F-2	VT	A	M	VL	M	S	A	M−	A	?	?	A	A	S+	M−	S+	VT	VT	M−	A
F-1	T	A	S	VL	M+	S	A	M+	A	?	?	A	A	A	M−	A	A	T	M−	A
F-3	VT	A	S	VL−	S	S	A	M−	A	A	A	A	A	A	M−	A	A	T	M−	A

Not detected in any samples: As, Os, Co, Ge, Au, In, Ir, Mo, Ni, Pd, Ru, Ta, Sn, Ti, W, Zn, Zr.

F-4: Argo. mine. Fine grained. Blue. Wallrock, Silver Plume granite. Pitchblende present (minor). In zone.

F-2: Brown Spar mine. Massive. Purple. Wallrock, Tertiary granodiorite. In zone.

F-1: Blue Jay mine. Massive. Purple-black. Wallrock, Tertiary granodiorite. In vein. Minor pitchblende in vein.

F-3: Caledonia mine. Crystalline. Purple-black. Wallrock, Silver Plume granite. In pyritic-gold vein.

Explanation of symbols

Symbol	Spectrographic Quantity Present	
A	Not detected	
VT	Very small trace	(Variations within one range ex-
T	Trace	pressed by plus and minus signs)
S	Small	
M	Medium	
L	Large	
VL	Very large	

Twenty minor elements were detected in the samples, and seventeen were absent in all. Other elements were not determined. Correlations between the minor elements present and a number of other factors were attempted. For instance, do the minor elements have any relation to the color of the fluorites? The only possible relation, as seen from Table 1, is that the "purple-black" samples contain less Mg, Mn, and Pb than the lighter-colored samples. However, there is nothing to prove that the coloring is due to the presence or absence of the elements. In fact, a better explanation of the difference in content of Mn, Mg, and Pb probably lies in the geological environment of each fluorite. The light-colored fluorites were formed in the older zones whereas the darker ones were formed in the younger veins.

Correlation with the type of wallrock, grain size of sample, nearness to the parent stock, age, vein type (i.e., fluorite vein, pyritic-gold vein, etc.), metallic minerals present in the deposit, radioactivity, and fluorescence was also attempted. As for age and nearness to the parent stock, the same can be said as for geologic environment. That is, certain differences in content of minor elements (Mg, Mn, and Pb) appear to be associated either with age of the deposit, its areal position relative to the source rock, the structural environment, or to all of these factors. A noteworthy fact is that the vein fluorites do not contain larger quantities of any minor element than the zone fluorites. The latter however contain a greater number of minor constituents than the vein fluorites.

The fine-grained sample (also the oldest), F-4, is by far the most impure of any analyzed. This may be due to the fact that quick chilling may have caused minor impurities to be incorporated in the crystallizing mass either as ions in the individual crystals, or as foreign mineral fragments between the tiny fluorite grains. This fine-grained sample bears more Na, Ba, Al, Fe, and Si than all the others, and is the only one that contains K, Sc, La, Ce, Nd, V, Cr, and Be. The purest sample is F-3, youngest of the group.

No obvious correlation between the minor elements detected and the wallrock of the deposits is possible from the data of Table 1, although the wallrocks contain abundant Sr and Ba (Bray, 1942 *a*). The minor constituents show no relation to the occurrence of pitchblende. As for the the fluorescent properties, the writer tested the samples under the light of an iron arc, with negative results in all cases. The data do not permit exact correlations with vein type or nature of metallic minerals present. The two samples in which Pb was detected were from deposits containing minor galena, but one sample in which no Pb was detected also came from a deposit bearing galena.

The most general and abundant minor elements present are Sr, Ba,

Fe, Y, Cu, Mg, Al, and Si. Sodium is not abundant and K was detected in only one sample. Does this fact indicate that the solutions depositing the fluorite were of an acid character (the usual belief)? In regard to the content of Sr and Ba, it has already been pointed out that these elements are abundant in the wallrocks. The rock with which the deposits are associated, the granite-quartz monzonite, is especially high in Sr and Ba (Bray, 1942 *a*).

TABLE 2. IONIC RADII OF THE ELEMENTS PRESENT*

Element	Group of Periodic System	Atomic Number	Atomic Weight	Valence	Ionic Radius (Å)
Na	I	11	22.99	1	0.98
Mg	II	12	24.32	2	0.76
Ca	II	20	40.08	2	1.06
Sr	II	38	87.63	2	1.27
Ba	II	56	137.36	2	1.43
Al	III	13	26.97	3	0.57
Y	III	39	88.92	3	1.06
Si	IV	14	28.06	4	0.39
Fe	Transition	26	55.84	2	0.83
Fe	Transition	26	55.84	3	0.67
Cu	I-B	29	63.57	1	0.96
Pb	IV-B	82	207.22	2	1.32

* Data obtained from Crystal Chemistry, by Stillwell, McGraw-Hill Book Co., **(1938)** (see appendix).

Table 2 lists the ionic radii of the elements of major importance to this discussion. It is notable that Y and Ca have identical radii, that Cu and Na have radii very near to that of Ca, and that only two of the elements listed have radii greater than that of Ca. These facts agree well with the conclusions drawn for silicate minerals of the Jamestown district (Bray, 1942 *a*; 1942 *b*), that most minor elements in ionic crystals probably occur as solid solution substitutes for major ions of like size in that structure. Some of the smaller ions, such as Si, may occur in interstitial solid solution. The strong affinity of Sr for Ca has been emphasized by several workers (Noll, 1934; Bray, 1942 *a* and 1942 *b*). Tröger (1935) has stated (with regard to the silicates) that rare-earth elements probably substitute for Ca because of similarity in their ionic radii. The same is

probably true here. It is interesting to see Tröger's statement borne out here with regard to Y in all analyses, and with regard to a number of other rare earth elements in analysis F-4. The reason Na is not more abundant in the fluorites, despite its similarity to Ca in ionic radius, is that it probably was not abundant in the fluorite-forming solutions.

Summary and Conclusions

Conclusions based on spectrographic analyses of four fluorite samples from Jamestown, Colorado, can be stated as follows:

1. There apparently is some relation between the minor elements detected in the fluorites and their geologic environments. Age of the deposit, areal position in relation to the parent stock, and type of deposit (vein or zone) can be included under environment.

2. No correlation exists between the minor elements present in the fluorites and the wallrock of each deposit. The same is true for radioactivity. The samples do not fluoresce.

3. The most general and abundant minor elements detected were Sr, Ba, Fe, Y, Cu, Mg, Al, and Si. These elements probably substitute for Ca in the fluorite structure.

4. The scarcity of K and Na indicates that the solutions which deposited the fluorite were not alkaline.

5. The finest grained fluorite, also the oldest, was found to be most impure. The youngest fluorite, from a pyritic-gold vein, was the purest.

References

Ball, S. H., Geology of the Georgetown Quadrangle, Colorado: *U. S. Geol. Survey, Prof. Paper* **63,** 29–96 (1908).

Bray, J. M., Spectroscopic distribution of minor elements in igneous rocks from Jamestown, Colorado: *Bull. Geol. Soc. Am.*, **53,** 765–814 (1942 *a*).

———, Distribution of minor chemical elements in Tertiary dike rocks of the Front Range, Colorado: *Am. Mineral.*, **27,** 425–440 (1942 *b*).

Fenneman, N. M., Geology of the Boulder District, Colorado: *U. S. Geol. Survey, Bull.* **265** (1905).

Goddard, E. N., Influence of Tertiary intrusive structural features on mineral deposits at Jamestown, Colorado: *Econ. Geol.*, **30,** 370–386 (1935).

Lovering, T. S., Geologic history of the Front Range, Colorado: *Proc. Colo. Sci. Soc.*, **12,** No. 4 (1929).

———, and Goddard, E. N., Geologic map of the Front Range mineral belt, Colorado (Explanatory Text): *Proc. Colo. Sci. Soc.* **14,** No. 1, 3–48 (1938).

———, and Goddard, E. N., Geologic map of the Front Range mineral belt, Colorado: *U. S. Geol. Survey*, Map (1939).

Noll, W., Geochemie des Strontiums: *Chemie der Erde*, **8,** 507 (1934).

Strock, L. W., Spectrum Analysis with the Carbon Arc Cathode Layer: *Adam Hilger Publication, London* (**1936**).

Tröger, E., Der Gehalt an selteneren Elementen bei Eruptivgesteinen; *Chemie der Erde*, **9** (3), 286–310 (1935).

NOTES AND NEWS

SPECTROGRAPHIC DATA CONCERNING THE PRESENCE OF THE LESS COMMON ELEMENTS IN ROCKS

GERALD O. FREEMAN, *Laucks Laboratories, Inc., Seattle, Washington.*

During a period of a little more than a year, from May 1941 to June 1942, 425 miscellaneous samples of rocks were analyzed spectrographically by Laucks Laboratories, Inc. Since the samples were collected and submitted for paid analysis by persons not connected with the laboratories, more than a cursory megascopic classification was not possible and data concerning locality were so slight as to be of little value. However, the results obtained are interesting and may be of value to future research.

The instrument used for the analysis is an Applied Research grating spectrograph, the 2″ original grating being ruled with 48,000 lines, giving a dispersion of 7 Å per mm. in the first order and a resolving power of .1 Å at 2400 Å. The samples were prepared by grinding to about an 80 mesh size, mixing and cutting until approximately 5 grams were obtained, and further grinding to a −200 mesh size. Two portions of the −200 mesh sample were burned between carbon electrodes, using a 10 ampere current at 220 volts D.C. with the lower electrode positive. Ten mg. were mixed with an equal amount of carbon and completely volatilized and 30 mg. were arced for 15 seconds. Only a sampled portion of the light from the first burning reached the film while it was exposed continuously to the 15-second arcing to insure the detection of the more volatile elements. The resulting spectrograms, which included the region between 2360 Å and 4600 Å, were studied with the aid of an Applied Research projection comparator, enabling quick and thorough analyses.

No element was reported present in a sample unless its presence was definitely established. Conversely, failure to report an element meant that it was not present in quantities above the limits of detection.

Possible extraneous sources of impurities were studied to determine their contaminative value. Periodic analyses of the carbon electrodes show that they do not interfere, with the possible exception of faint Cu lines. The amount of Cu in the samples, however, is in nearly every case greater than the amount added by the electrodes. Contamination by the grinding apparatus is slight, being confined to an addition of a trace of Fe to the sample. Dust in the air is a possible source of error, but tests have shown this to be almost nonexistent.

Because of their abundance and common presence in the majority of rocks, Si, Ca, Mg, Al, Na, K, Fe are not listed in this study. All except

Na and K were found in every sample studied and the latter two were found in a majority of cases.

Table 1 gives data concerning the amounts of elements detectable, using the above procedure, in a silica base. The limits tend to vary with the base used, i.e. from rock to rock, however, the variation seems to be slight in most cases.

Spectrographic Data

Table 1. Table Showing Limits of Detection of the Elements Found in the Studied Samples, in a SiO_2 Base

Element	Limit of Detection	Element	Limit of Detection	Element	Limit of Detection	Element	Limit of Detection
	(less than)		(less than)		(less than)		(less than)
Cu	0.001%	Sn	0.001%	Mo	0.001%	Ge	0.01%*
Ti	0.001%	Co	0.001%	As	0.1%	Pt	0.001%
V	0.001%	Sr	0.001%	Sb	0.1%	Te	0.1%
Cr	0.001%	Ag	0.001%	Cd	0.01%	Y	0.1%
Mn	0.001%	Ga	0.01%*	Au	0.01%	Ru	?
Ni	0.001%	Zr	0.01%	W	0.1%	Cb	?
Ba	0.001%	Zn	0.01%	In	0.01%*	Li	?
Pb	0.001%	Bi	0.001%	Be	0.001%		

* Probably.

Table 2. Table Showing the Number of Occurrences of the Elements in the Rocks Studied and Their Per Cent Occurrence

Element	No. of Samples	% of Total	Element	No. of Samples	% of Total	Element	No. of Samples	% of Total
—	425	100	Sr	312	73	W	4	1
Cu	418	99	Ag	274	64	In	3	0.7
Ti	416	98	Ga	192	45	Li	2	0.5
V	413	97	Zr	158	37	Cb	2	0.5
Cr	411	97	Zn	141	33	Ge	2	0.5
Mn	408	96	Bi	107	25	Be	1	0.2
Ni	408	96	Mo	52	12	Pt	1	0.2
Ba	408	96	As	43	10	Ru	1	0.2
Pb	401	95	Sb	39	9	Te	1	0.2
Sn	383	90	Cd	21	5	Y	1	0.2
Co	364	83	Au	7	2			

Tables 2 and 3 give data concerning the presence of elements in the miscellaneous samples analyzed. The classification is necessarily very general. "Acid Igneous" includes the granitic and dioritic rocks and their extrusive equivalents; "Basic Igneous" includes basalts, gabbros, pyrox-

enites, amphibolites and similar rocks; "Magnetite" includes only massive magnetite; "Hydrothermal" refers to all rocks apparently formed by deposition from circulating waters; and "Miscellaneous" includes all samples which could not be classified, such as submitted, previously ground samples, rocks of such complexity as to preclude any definite classification, and rock mixtures.

TABLE 3. TABLE SHOWING THE NUMBER OF OCCURRENCES OF THE ELEMENTS IN THE ROUGHLY CLASSIFIED SAMPLES

Element	Acid Igneous	Basic Igneous	Magnetite	Hydrothermal	Sands and Sandstone	Shale	Limestone	Misc. Sedimentary	Metamorphic	Miscellaneous
No. of samples	47	34	13	84	36	51	16	15	51	78
Cu	47	34	13	84	35	48	16	15	50	76
Ti	47	32	13	84	36	51	16	15	50	72
V	43	33	13	82	36	50	14	15	50	77
Cr	46	34	12	78	35	50	15	13	51	78
Mn	46	34	13	74	33	50	15	15	51	77
Ni	45	33	13	78	35	50	13	13	51	77
Ba	45	33	13	81	34	51	16	14	50	71
Pb	47	33	11	80	34	46	16	13	50	71
Sn	47	33	11	73	32	42	14	11	48	72
Co	43	31	12	58	32	49	11	11	49	68
Sr	40	30	2	52	27	44	15	9	36	57
Ag	32	24	8	38	24	36	7	7	37	61
Ga	37	23	1	12	19	32	7	4	21	36
Zr	31	8	1	5	21	30	5	4	18	35
Zn	8	9	7	45	9	8	1	6	19	29
Bi	13	5	4	35	7	7	3	3	12	18
Mo	8	2	2	6	3	4	1	2	7	17
As	2	1	—	25	1	2	1	—	2	8
Sb	4	1	—	19	4	2	2	1	—	6
Cd	2	—	—	14	—	—	—	—	—	5
Au	—	—	—	3	2	—	—	—	—	2
W	—	—	—	2	—	1	—	—	—	1
In	—	—	—	2	—	—	—	—	—	1
Be	1	—	—	—	—	—	—	—	—	—
Cb	1	—	—	—	—	—	—	—	1	—
Ge	—	—	—	1	—	—	—	—	—	1
Li	1	—	—	—	—	—	—	—	1	—
Pt	—	—	—	—	1	—	—	—	—	—
Ru	1	—	—	—	—	—	—	—	—	—
Te	—	—	—	—	1	—	—	—	—	—
Y	—	—	—	1	—	—	—	—	—	—

Comments

1. The Y was found in a sample determined to be about 50 per cent fluorite and 40 per cent quartz.

2. The Te occurred in a sample of sand which also contained Au and Bi.

3. A trace of Pt was found in a sample of sand only after analysis of an assay bead.

4. Ge was found in a sample of a mixture of pyrite and quartz which also contained Pb, As, Zn, and Cd and a sample of pulp in which there was approximately 5 per cent Zn.

5. Be was found in a granitic appearing rock which had been altered by weathering.

6. The In occurred in samples containing Zn and Pb, always with more Zn than Pb.

7. In only two samples is Cd found and Zn not reported. Both are classified as acid igneous rocks.

8. Cb occurred in a large crystal of orthoclase which also contained traces of Li and Ru besides the usual trace elements, and a sample of schist, which also contained Li. Neither sample was otherwise obviously unusual.

9. The elements which are most often found are those which can be detected in the smallest amounts.

Due to the nature of the data, conclusions are not feasible, so that an attempt has been made only to summarize the results obtained over a long period of time by the use of the spectrograph.

BOOK REVIEW

X-RAY CRYSTALLOGRAPHY, AN INTRODUCTION TO THE INVESTIGATION OF CRYSTALS BY THEIR DIFFRACTION OF MONOCHROMATIC *X*-RADIATION, by M. J. BUERGER, Associate Professor of Mineralogy and Crystallography, Massachusetts Institute of Technology. New York, John Wiley and Sons, Inc.; London, Chapman and Hall, Ltd., 1942. Pp. xxii+531, figs. 252, and end-paper diagrams. 6″×9″. Cloth. Price $6.50.

Professor Buerger states that this book is devoted to the geometry of the space patterns in crystals; it thus deals with the crystal class, the space lattice (its type and dimensions), and the space group. The field so delimited is one not previously treated with sufficient fullness in any one book to meet practical needs; the author covers it very thoroughly and his book will be very useful to all those having to investigate crystals with *x*-rays, either as a part of the determination of an atomic arrangement or in the course of systematic crystallographic studies.

The moving film methods, which permit the straightforward determination of the geometric properties mentioned above, occupy the largest part of the book. They include the Weissenberg method, the Sauter method, the Schiebold method, and the DeJong and Bouman method. The earlier rotation and oscillation methods are also discussed in detail. The equi-inclination Weissenberg method receives the largest amount of space devoted to any one method; the reviewer considers this to be in keeping with its comparative utility. In a section entitled "Advantages of taking Weissenberg photographs by the equi-inclination method" Professor Buerger writes "it is uniquely possible for the equi-inclination method to record central lattice rows as straight lines, and thus permit easy reconstruction of the reciprocal lattice, and also, more generally, to record the lattice rows of all layers as curves of similar shape, and consequently permit indexing directly on the film." These important advantages of the equi-inclination method he discovered several years ago. Additional advantages of the equi-inclination Weissenberg method over the methods involving perpendicular incidence might well have been mentioned explicitly at this point; for example, with the equi-inclination method there is no blind area around the rotation axis in any reciprocal lattice layer so that no planes of low indices fail to register on the diffraction photographs.* Besides the chapters devoted to experimental methods, others are devoted to: Some Geometrical Aspects of Lattices; The Diffraction of *X*-Rays by Crystals; Space-Group Extinctions; The Reciprocal Lattice; Geometrical Interpretation of Bragg's Law: Application of the Reciprocal Lattice to the Solution of *X*-Ray Diffraction Problems; The Geometry of Oblique Cells and Their Reciprocals; The Experimental Determination of the Lattice Constants of the Crystals Belonging to the Oblique Systems; The Theory of Attaining Precision in the Determination of Lattice Constants; The Precision Determination of the Linear and Angular Lattice Constants of Single Crystals; The Theory and Interpretation of Reciprocal Lattice Projections. The ionization spectrometer method introduced by the Braggs is not discussed, although it was the first method by means of which the dimensions of the unit cell could be rigorously determined and the *x*-ray diffraction effects unambiguously indexed. It also has an important practical application at the present time.

Under the heading "The choice of elements and setting of a triclinic crystal" three rules are given for attainment of a unique setting. Unfortunately these rules cannot be

* Analysis of intensities is left outside the scope of the book, but since some mention is made of intensity factors it may be noted in passing that it has been shown by the reviewer that the equi-inclination method possesses equally important advantages in respect to the intensities of the diffraction spots.

applied in all cases. Progress toward the result aimed at has undoubtedly been made by Professor Buerger and other crystallographers in recent years and it is reasonable to hope that agreement on suitable rules may be reached in the near future.

A section of great mathematical elegance is that of the interpretation of x-ray photographs by means of plane-groups, one of Professor Buerger's own contributions.

The author points out that the term *lattice* is frequently misused at the present time. The term properly means an array of points in space produced by periodic translational repetition of an original point. He rightly states that the term *lattice* should not be construed to mean the actual material crystal structure of packed atoms.

The author's terminology is not altogether felicitous in a few places. For instance, *symmetry operations* are called "elements of repetition" (p. 2); the new term "line lattice" is used with two different meanings (p. 4 and p. 34); the *symbol* of three *indices* (*hkl*) is called the "index."

In conclusion, it may be stated that a large number of excellent line drawings and halftone reproductions of x-ray photographs will assist the reader to grasp with a minimum of effort the rather complicated geometrical relations involved in x-ray crystallography.

The material presentation of the book is up to Wiley's usual high standard. The small number of typographical errors can easily be corrected in the next printing.

GEORGE TUNELL

Geophysical Laboratory,
Carnegie Institution of Washington,
Washington, D. C.

Cancellation of Ottawa Meeting

Because of the war and the attendant difficulties, bringing increased burdens upon the membership of the society, together with the difficulties of travel and arranging accommodations, the Council of the Mineralogical Society of America has voted to cancel the meeting originally scheduled for Ottawa, December 29–31, 1942. This follows the action of the Council of the Geological Society of America which has cancelled the concurrent meeting of that society.

Abstracts for papers to be published will be received as usual, but publication of the official program for the annual meeting will be omitted this year. Abstracts submitted will be published in the March issue of the journal along with the report on the affairs of the society for 1942.

Paul F. Kerr, *Secretary*